

**REPORT DOCUMENTATION PAGE**

*Form Approved  
OMB No. 0704-0188*

The public reporting burden for this collection of information is estimated to average 1 hour per response, including the time for reviewing instructions, searching existing data sources, gathering and maintaining the data needed, and completing and reviewing the collection of information. Send comments regarding this burden estimate or any other aspect of this collection of information, including suggestions for reducing the burden, to Department of Defense, Washington Headquarters Services, Directorate for Information Operations and Reports (0704-0188), 1215 Jefferson Davis Highway, Suite 1204, Arlington, VA 22202-4302. Respondents should be aware that notwithstanding any other provision of law, no person shall be subject to any penalty for failing to comply with a collection of information if it does not display a currently valid OMB control number.  
**PLEASE DO NOT RETURN YOUR FORM TO THE ABOVE ADDRESS.**

<b>1. REPORT DATE (DD-MM-YYYY)</b> 5/8/2019			<b>2. REPORT TYPE</b> MASTERS THESIS		<b>3. DATES COVERED (From - To)</b> JULY 2017 - MAY 2019	
<b>4. TITLE AND SUBTITLE</b> USE OF AN ASYMMETRIC PROPELLER FOR UNMANNED UNDERWATER VEHICLES					<b>5a. CONTRACT NUMBER</b>	
					<b>5b. GRANT NUMBER</b>	
					<b>5c. PROGRAM ELEMENT NUMBER</b>	
<b>6. AUTHOR(S)</b> ROBERT BELTRI CARELLI					<b>5d. PROJECT NUMBER</b>	
					<b>5e. TASK NUMBER</b>	
					<b>5f. WORK UNIT NUMBER</b>	
<b>7. PERFORMING ORGANIZATION NAME(S) AND ADDRESS(ES)</b> MASSACHUSETTS INSTITUTE OF TECHNOLOGY, 77 MASSACHUSETTS AVE, CAMBRIDGE, MA 02139					<b>8. PERFORMING ORGANIZATION REPORT NUMBER</b>	
<b>9. SPONSORING/MONITORING AGENCY NAME(S) AND ADDRESS(ES)</b>					<b>10. SPONSOR/MONITOR'S ACRONYM(S)</b>	
					<b>11. SPONSOR/MONITOR'S REPORT NUMBER(S)</b>	
<b>12. DISTRIBUTION/AVAILABILITY STATEMENT</b> DISTRIBUTION A						
<b>13. SUPPLEMENTARY NOTES</b>						
<b>14. ABSTRACT</b> This thesis describes the development and execution of a test program to determine the suitability of an asymmetric propeller for unmanned underwater vehicles (UUV). Woods Hole Oceanographic Institute reevaluated the concept for use on a UUV, but for two different objectives. The first was a possible improvement in propulsive efficiency. By controlling the speed of the propeller through each revolution, the thrust at any given point can be controlled. This allows for a non-uniformly distributed thrust about the longitudinal axis of the UUV which can be used to steer the UUV.						
<b>15. SUBJECT TERMS</b>						
<b>16. SECURITY CLASSIFICATION OF:</b>			<b>17. LIMITATION OF ABSTRACT</b> UNCLASS	<b>18. NUMBER OF PAGES</b> 83	<b>19a. NAME OF RESPONSIBLE PERSON</b> ROBERT BELTRI CARELLI	
<b>a. REPORT</b> UNCLASS	<b>b. ABSTRACT</b> UNCLASS	<b>c. THIS PAGE</b> UNCLASS			<b>19b. TELEPHONE NUMBER (Include area code)</b> 617-253-4339	

THIS PAGE INTENTIONALLY LEFT BLANK

USE OF AN ASYMMETRIC PROPELLER FOR  
UNMANNED UNDERWATER VEHICLES

by

Robert Beltri Carelli

B.S. Naval Architecture and Marine Engineering, Webb Institute (2009)

Submitted to the System Design and Management Program and

Department of Mechanical Engineering

in partial fulfillment of the requirements for the degrees of

Master of Science in Engineering and Management

and

Naval Engineer

at the

MASSACHUSETTS INSTITUTE OF TECHNOLOGY

June 2019

© Massachusetts Institute of Technology 2019. All rights reserved.

Author  .....

System Design and Management Program and Department of  
Mechanical Engineering

May 18, 2019

Certified by  .....

Eric Rebentisch  
Research Associate, Sociotechnical Systems Research Center  
Thesis Supervisor

Certified by  .....

Alexandra Techet  
Professor of Ocean & Mechanical Engineering

Thesis Supervisor

Accepted by  .....

Joan S. Rubin  
Executive Director, System Design and Management

Accepted by  .....

Nicolas Hadjiconstantinou  
Chairman, Department Committee on Graduate Theses

*[Faint, illegible handwritten signature or scribble]*

# USE OF AN ASYMMETRIC PROPELLER FOR UNMANNED UNDERWATER VEHICLES

by

Robert Beltri Carelli

Submitted to the System Design and Management Program and Department of  
Mechanical Engineering  
on May 18, 2019, in partial fulfillment of the  
requirements for the degrees of  
Master of Science in Engineering and Management  
and  
Naval Engineer

## Abstract

This thesis describes the development and execution of a test program to determine the suitability of an asymmetric propeller for unmanned underwater vehicles (UUV). The idea to utilize a single blade propeller had been pioneered in the past for aviation as an attempt to generate greater thrust, but was quickly abandoned. Recently, Woods Hole Oceanographic Institute reevaluated the concept for use on a UUV, but for two different objectives. The first was a possible improvement in propulsive efficiency. For UUVs meant to operate for long periods without recharging, any increase in propeller efficiency can result in more time on station. The second object was to allow for an alternate method of steering the UUV. By controlling the speed of the propeller through each revolution, the thrust at any given point can be controlled. This allows for a non-uniformly distributed thrust about the longitudinal axis of the UUV which can be used to steer the UUV.

This thesis evaluated the efficiency of using such a propeller. This data was used to determine the suitability for UUVs and in which use cases an asymmetric propeller used for propulsion and steering. Due to issues during testing the control authority provided along a variety of speeds could not be determined for comparison to a traditional propeller and rudder configuration.

Thesis Supervisor: Eric Rebentisch

Title: Research Associate, Sociotechnical Systems Research Center

Thesis Supervisor: Alexandra Tchet

Title: Professor of Ocean & Mechanical Engineering



## Acknowledgments

As I finish my time here at MIT, I wanted to take this opportunity to thank all the people who helped me along the way.

First, my thesis advisers who helped me plan and execute this project. Professor Techet, thank you for the technical guidance and support building testing the propeller boat. Professor Rebentisch, thank you for agreeing to supervise this thesis and helping me take on a very technical thesis and adapt the project to allow me to incorporate the knowledge from the SDM program to create a more meaningful end product.

Next, I would like to thank Mark Belanger for all the time he dedicated teaching me to use all the tools at the Edgerton student shop and his assistance throughout the construction of the propeller boat. I am confident that I would not have succeeded in building a functioning propeller boat without the amount of help and knowledge he offered throughout the process.

I was fortunate enough to have aligned my thesis with Bill Hetschel who was working on a different aspect of propeller testing. Working with him to construct the propeller boat was a tremendous asset and I appreciate having someone to work through the numerous problems with. I also appreciate the continued support he provided towards my thesis after he had concluded his testing.

Finally, thank you to my wife and the rest of my family for their continued support both in getting here and throughout my time at MIT.

THIS PAGE INTENTIONALLY LEFT BLANK

# Contents

<b>1</b>	<b>Introduction</b>	<b>13</b>
1.1	Project Motivation . . . . .	13
1.2	Research Question . . . . .	14
1.2.1	Research Approach . . . . .	15
<b>2</b>	<b>Background</b>	<b>17</b>
2.1	History of Drone Development . . . . .	17
2.2	Challenges for Designing UUVs . . . . .	18
2.3	Drone Usage withing the Department of Defense . . . . .	20
2.4	Historical Use of Single Blade Propellers . . . . .	21
2.4.1	Development of Single Blade Propellers for Aircraft . . . . .	22
2.4.2	Single Blade Propeller Development by WHOI . . . . .	23
2.5	Summary . . . . .	24
<b>3</b>	<b>Stakeholder analysis</b>	<b>25</b>
3.1	Distributed Lethality Concept and the Role of UUVs . . . . .	25
3.2	Requirements for future UUVs . . . . .	27
3.3	Decomposition of a UUV . . . . .	29
3.4	Use Case for Asymmetric Propeller . . . . .	30
3.4.1	Benefits . . . . .	30
3.4.2	Trade Offs . . . . .	34
3.4.3	Summary . . . . .	35

<b>4</b>	<b>Test Program</b>	<b>37</b>
4.1	Overview . . . . .	37
4.2	Open Water Test Theory . . . . .	37
4.3	Propeller Boat Design . . . . .	41
4.3.1	Propeller Boat Tradespace . . . . .	42
4.4	Propeller Boat Detail Design and Construction . . . . .	45
4.4.1	Sensor Selection and Placement . . . . .	48
4.5	Propeller Boat Validation Process . . . . .	52
4.6	Propeller Boat Validation . . . . .	53
4.7	Single Blade Propeller Propulsive Testing . . . . .	55
4.8	Control Authority Testing . . . . .	57
4.8.1	Model Self-Propulsion Tests . . . . .	57
4.8.2	Modification for Control Authority Testing . . . . .	58
<b>5</b>	<b>Results</b>	<b>61</b>
5.1	Open Water Propeller Test Results . . . . .	61
5.2	Control Authority Results . . . . .	64
<b>6</b>	<b>Conclusion</b>	<b>67</b>
6.1	Feasibility and Desirability for UUVs . . . . .	67
6.1.1	Efficiency . . . . .	67
6.1.2	Control Authority . . . . .	69
6.1.3	Summary . . . . .	69
6.2	Future Recommendations . . . . .	69
<b>A</b>	<b>Control Authority Estimation</b>	<b>71</b>
<b>B</b>	<b>Propeller Boat Validation Test Results</b>	<b>73</b>
<b>C</b>	<b>Single Blade Propeller Test Results</b>	<b>79</b>

# List of Figures

1-1	Typical propeller configurations . . . . .	13
1-2	System Engineering Design Process [5] . . . . .	15
2-1	2016 Drone Usage in the United States . . . . .	18
2-2	Single propeller UUVs (Konsberg: left, Riptide: right) . . . . .	19
2-3	Multiple thruster UUVs, BAE Talisman (left) and Balt Robotics (Right)	20
2-4	CONOPS for UUV integration to fleet operations . . . . .	21
2-5	Everel propeller mounted on a J-2 Cub aircraft . . . . .	23
2-6	Single blade propeller functional concept . . . . .	24
3-1	UUV Master plan vision for future warfare areas [4] . . . . .	26
3-2	Formal decomposition of UUVs with control surfaces (left) and asym- metric propeller (right) . . . . .	29
3-3	Mapping of performance attributes to UUV design . . . . .	30
3-4	Mode of operation for control surfaces . . . . .	31
3-5	Control authority comparison . . . . .	32
3-6	B Series propeller efficiency . . . . .	33
3-7	B-series propeller thrust . . . . .	34
4-1	ITTC test setup overview [1] . . . . .	38
4-2	Open water propeller test rig setup [1] . . . . .	39
4-3	Propeller fairing recommendations from ITTC [1] . . . . .	39
4-4	Open water propeller test sample results . . . . .	41
4-5	Possible test setup architectures . . . . .	44

4-6	Rendering of propeller boat design . . . . .	45
4-7	Propeller shaft with support plates shown with and without T-slotted aluminum . . . . .	46
4-8	Final lower structure with nosecone . . . . .	47
4-9	Final upper structure configuration . . . . .	47
4-10	MIT tow tank and carriage . . . . .	48
4-11	Final propeller boat configuration mounted to tow carriage . . . . .	49
4-12	Kistler gage information flowpath . . . . .	49
4-13	AMTI strain gauge information flowpath . . . . .	50
4-14	Thrust sensor configuration - Initial (top) and Final (bottom) . . . . .	51
4-15	Validation test results, expected values shown by orange lines . . . . .	54
4-16	Regression for data from validation testing . . . . .	55
4-17	Aluminum propeller used for 1-blade propeller testing . . . . .	56
4-18	Model self-propulsion test setup guidelines from ITTC . . . . .	57
4-19	Rudder (left) and propeller (right) control systems . . . . .	58
4-20	Configuration for control authority testing [3] . . . . .	59
5-1	Initial test results for single blade propeller . . . . .	62
5-2	Open water test results . . . . .	63
5-3	Open water performance comparison for one and two blade propellers	64
6-1	Operating point comparison . . . . .	68

# List of Tables

3.1	Mission pillars for UUVs [4]	27
3.2	Performance comparison against traditional cylindrical UUV	35
4.1	Test Rig Design Tradespace	43
4.2	Validation test matrix	53
4.3	Single blade propeller test matrix	56

THIS PAGE INTENTIONALLY LEFT BLANK

# Chapter 1

## Introduction

### 1.1 Project Motivation

Propeller design has long been a focus for watercraft for both surface or subsurface vehicles. However, the focus has traditionally been on how to improve the propeller performance such as increasing efficiency and creating more thrust. Since the introduction of the screw propeller, different architectures have been developed such as shrouded propellers, new blade designs, waterjets, and counter rotating configurations some of which are shown in Figure 1-1.

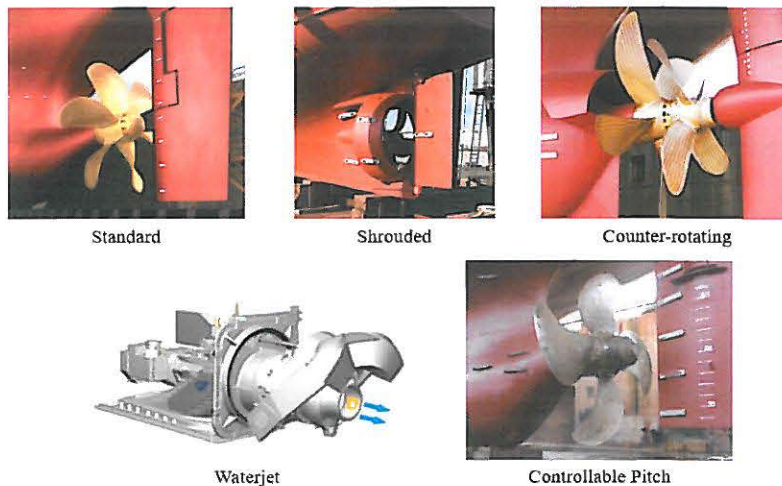


Figure 1-1: Typical propeller configurations

Each of these designs was made to optimize the propulsive efficiency in some manner. For example, the waterjet is inefficient at low speeds, but more efficient than conventional propellers at high speeds making it optimal for high speed vessels such as catamaran ferries. The shrouded propeller allows for higher efficiency with a smaller propeller by reducing the losses at the blade tips. A controllable pitch propeller allows the prime mover to operate at its ideal speed and controls the pitch to create the required amount of thrust.

When the prevalence unmanned underwater vehicles (UUV) began to grow, they largely adopted the standard propulsion and control systems which are found on larger ships. However, due to the operating constraints on these vehicles, it is possible that a different architecture could provide a more robust solution than adopting current designs to meet the need.

Preliminary testing conducted by Woods Hole Oceanographic Institute (WHOI) demonstrated that through the use of an asymmetrical propeller, a UUV is capable of being propelled and maneuvered using the same system. With a proof of concept completed showing a single blade propeller can serve to power and steer a small UUV, this thesis aimed to conduct more rigorous and controlled testing. This thesis provided a baseline for the performance of an asymmetrical propeller and evaluated what the requirements are for a UUVs in today's missions and missions of the future and how they can be met by using an asymmetric propeller.

## 1.2 Research Question

Through this thesis I evaluated the performance characteristics as well as feasibility and desirability of a single bladed propeller for use on UUVs. The overall process focused on three research questions:

1. How does the performance of a single bladed propeller compare to a multi-blade propeller of a similar design
2. What design attributes will be effected when using a single blade propeller and

what are the tradeoffs between the two alternative

3. What is the appropriate use case for a single blade propeller

### 1.2.1 Research Approach

For this thesis I utilized the system engineering approach to ensure a thorough analysis of the utility of a single bladed propeller for UUVs. This approach, shown in Figure 1-2, consists of two simultaneous processes. The first is to validate the requirements for the system and the second is to verify the product is meeting the needs of the system.

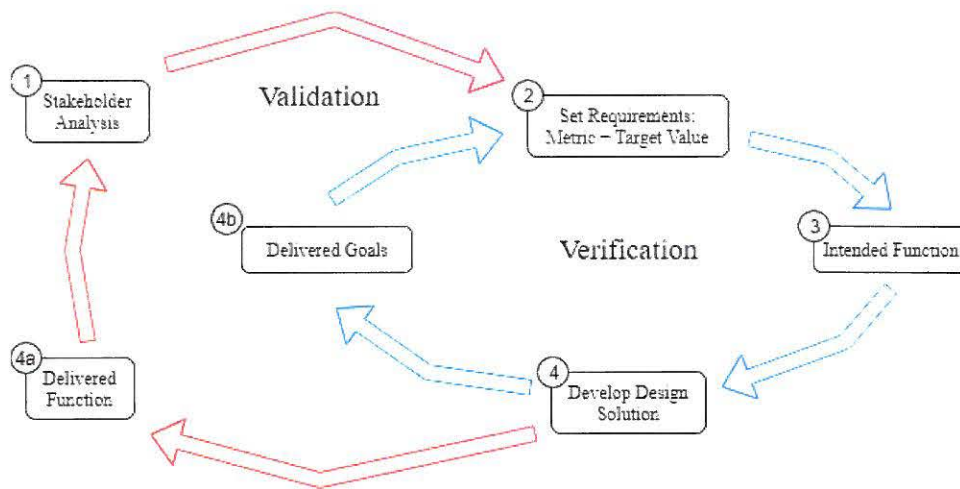


Figure 1-2: System Engineering Design Process [5]

1. Stakeholder analysis - The first step in the process was to evaluate who the primary beneficiaries are for the UUVs currently in use and for those in the future. This was accomplished through research of the drone industry to determine where the technology could best be implemented and who it would impact.
2. Set Requirements - Based on the stakeholders identified in the first part of the process, I selected where the technology is going to be implemented and what the operating condition would be. This allowed me to develop attributes which can be used to evaluate the success of the design.

3. Intended Function - Using information from previous uses of single bladed propellers and recent preliminary testing I outlined the intended function for modern UUVs.
4. Implement Design Solution - In this case, the design solution being evaluated has been identified and needed to be implemented. I instead addressed how the single bladed propeller will be incorporated into a UUV and the impact it will have on the operations of the UUV.
  - (a) Evaluate delivered Function - In order to determine the delivered function of the single bladed propeller, I developed and executed a test program to determine the operating parameters. These results were compared to a conventional propeller with similar blade design to allow for an accurate baseline.
  - (b) Evaluate delivered goals - Using the data obtained from part 4a, I was able to compare the results obtained to the desired attributes from the beginning of the process and determine the feasibility and desirability of implementing the new propulsion system. I was also able to look at the trade offs between the two alternatives to determine if there is a point where each the two technologies have comparable performance and in which regime each is superior. In this process, it was also important to evaluate any added benefits or issues which arose from the new technology.

# Chapter 2

## Background

### 2.1 History of Drone Development

Drones have been around since the early 1900s in the form of unmanned military airplanes, but they have become increasingly prevalent in recent history. [1] Over the past decade, drones have emerged as a means of extending the reach of our capabilities along numerous different sectors. They represent an alternate method to allow humans to accomplish goals that would be costlier and also more dangerous for humans if not impossible all together. Today drones are a ubiquitous sight from recreational quad copters to military aircraft used to fly missions in combat zones. While military investment represents the largest sector with over \$70 billion compared to \$17 billion for consumer drones and \$13 billion for commercial drones in 2016 [7], better and cheaper technology available today has increased their roll across several sectors. Figure 2-1 shows the usage of drones across different industries in the United States.

Unmanned aerial vehicles (UAVs) have been under development for a while, however, underwater drones have become more viable with the improvements in computing power and power storage. Because of this, aerial drones still represent a majority of the development to date, however there are several industries pushing for development of more capable underwater drones. Use of undersea vehicles has opened up operations that were previously not possible, such as working on subsea oil equipment

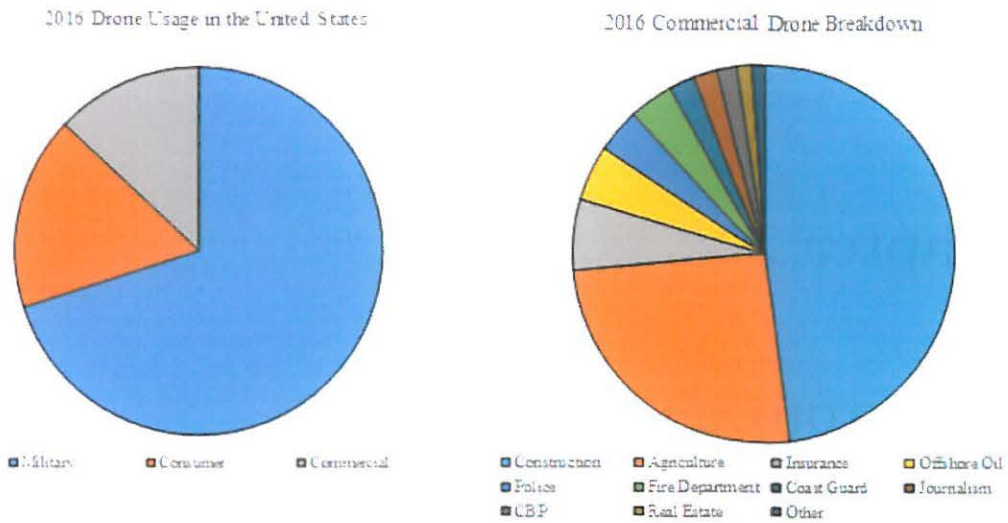


Figure 2-1: 2016 Drone Usage in the United States

at 10,000ft of depth. By removing the need for life support systems, they are able to operate well beyond the limits of manned vehicles without risking the operators at the same time. However, because of the operating environment, the challenges for UUVs are completely different from those facing UAVs.

## 2.2 Challenges for Designing UUVs

Of the many challenges that are specific to underwater operation, they can mostly be traced back to the the material properties of the fluid they operate in. Unlike air, water has a vastly higher density and is more opaque. This changes everything from how the UUV is propelled and maneuvered to how it communicates. [8]

The opaque nature of water makes the use of the sensors utilized for UAVs ineffective. The typical transmission range for optics in the ocean is under 300m. Similarly, active sonar for imagining has very limited ranges. UUVs cannot communicate while underwater due to the inability to transmit electromagnetic radiation through water. As a result, they often need to be able to operate for long periods of time autonomously to accomplish a mission in an area that a UAV could cover in a

significantly shorter amount of time.

The second distinguishing challenge, also a result of the increased density of the operating fluid, is that the drones face much higher resistance resulting in lower operating speeds. This impacts not only the size of an operating area a UUV can operate in but also what missions the UUV can accomplish because of its maneuverability. Over time, UUVs have mostly fallen into two major categories to overcome this issue. The first are long slender UUVs which have only one propeller and use foils to steer the UUV. This design evolved to prioritize hydrodynamics and compatibility with host ships. Some examples of this can be seen in Figure 2-2. This configuration is optimal for applications where a high degree of maneuverability is not required and utilizing a more compact UUV is desirable. The maneuverability of the UUV, will be proportional to the size of the control surfaces and the speed of the UUV. As discussed earlier, UUVs typically operate at relatively low speeds which will negatively impact the steering for a slender UUV. Increasing the size of the fins can overcome this, however there are other tradeoffs associated with this. From the examples shown in Figure 2-2, there are different ways increase the control surface size. The Hugin by Kongsberg has a reduced diameter near the control surfaces of the UUV which allows it to maintain the overall outer diameter. This allows for large control surfaces but reduces the internal volume of the UUV which limits the capacity for payload or batteries. The Riptide UUV has larger control surfaces which extend beyond the outer diameter of the UUV. This maximized the internal space and allowed for better hydrodynamic performance of the control surfaces, but increases the footprint of the UUV and limits methods of launch, recovery, and storage.



Figure 2-2: Single propeller UUVs (Kongsberg: left, Riptide: right)

The other dominant configuration uses multiple thrusters which are used for both propelling the UUV as well as maneuvering. Figure 2-3 shows some examples of UUVs which use vectored and differential thrust to maneuver. In this configuration, the UUV can achieve a higher degree of maneuverability without sacrificing internal volume. For this configuration, a wider vehicle will be preferable because it allows for better differential between propellers for more effective steering, however this results in a larger vehicle that may not be as convenient. The major trade off in these designs is the size of the vehicles. For instances where the UUVs are being included on existing platforms this can be particularly limiting. For example, UUVs which are launched from submarines must fit through one of the existing interface including torpedo tubes and hatches. This would preclude the use of many larger multi thruster UUVs for deployment from submarine platforms.



Figure 2-3: Multiple thruster UUVs, BAE Talisman (left) and Balt Robotics (Right)

## 2.3 Drone Usage withing the Department of Defense

As the largest investor in drone technology, it was important to look at the defense industry and how it has driven a lot of the development within the industry. As such, I have decided to focus on the role which UUVs play within the defense sector to understand the future of the technology. The US Navy completed a study and released a UUV Master Plan which outlines needs for UUVs as well as their use case for the future. This has been reinforced by a push in the Navy towards the need for a “distributed lethality.” In the future operations, high cost and high capability units will need to be supplemented by lost cost autonomous vehicles. The Navy UUV

Master Plan states that “UUV technology is a force multiplier to manned platforms and is essential to meet critical requirements. UUV technology [increases] timeliness and cost effectiveness.” [4] The UUV master plan states that vehicles need to be able to operate for autonomously for extended periods of time while coordinating with host units as shown in Figure 2-4.

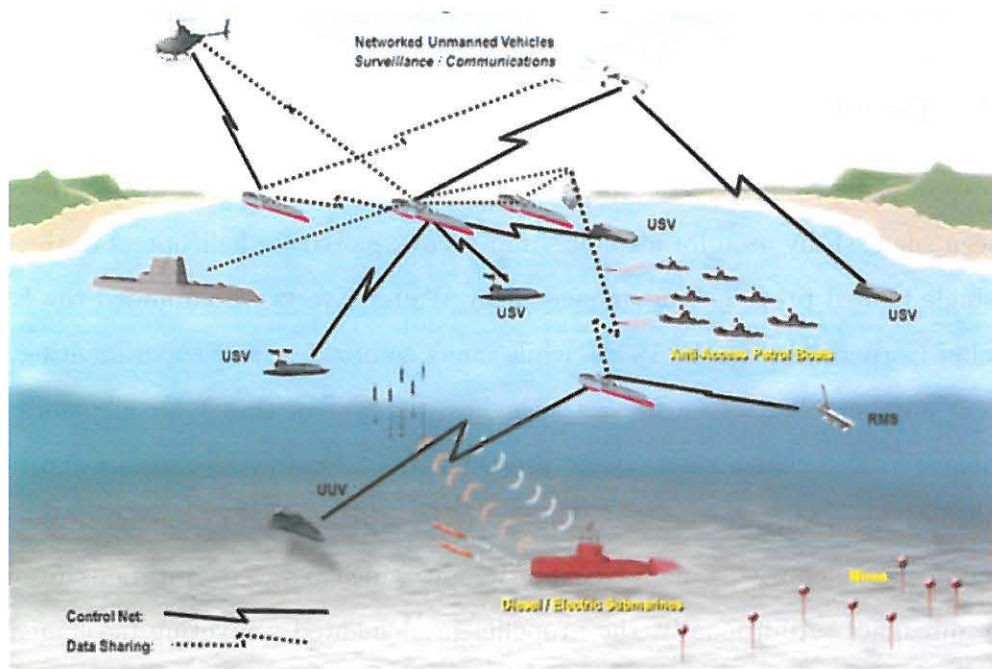


Figure 2-4: CONOPS for UUV integration to fleet operations

In its road map summary, the Navy states that the use of drones will “provide access to areas denied to manned platforms; provide better situational awareness; increase capabilities with greater range and persistence; and enable faster decision making” [4] To enable this, the Navy needs UUVs with more endurance and greater flexibility than what is currently available.

## 2.4 Historical Use of Single Blade Propellers

Based on the emphasis of developing UUVs for future DOD uses, I focused my thesis on the possibility of improving the propulsion for a UUV by implementing a new

type of propeller which could lead to a better suited UUV for certain operations. The single blade propeller could yield two areas of increased efficiency for a UUV operator, both in the propulsion of the UUV and in the maneuverability of the UUV through certain portions of its operating envelope. Prior to beginning my thesis, I researched prior uses of single bladed propellers to understand some of the issues and prior work which could help me construct a better test program.

### **2.4.1 Development of Single Blade Propellers for Aircraft**

The idea of using a single bladed propeller is new in the underwater field, however, it has been successfully used for airplanes and even explored for helicopters in the past. The single bladed propeller was pioneered by Walter Everts who founded the Everel Propeller Corporation. In the 1930s, while many companies were experimenting with different number blades to achieve the highest amount of thrust for airplanes, Everel demonstrated that a single blade propeller was a feasible alternative and began marketing it as a superior design. The Everell propeller, shown in Figure 2-5, was a wooden propeller with a metal counterweight which reduced vibrations from the blade imbalance. Additionally, the propeller implemented a pivoting mechanism on the hub designed to allow the propeller pitch to change under different loading conditions. The theory was that the propeller would use a coarse pitch during heavy loading and change to a fine pitch under lower loading conditions.

Everet's thought was that by using only a single blade, the blade would be operating in undisturbed air allowing the blade to generate more lift and for the propeller to produce more thrust. In 1937, an article by Arthur Pierce in the "The Sportsman Pilot" describes a cross country flight from Pennsylvania to the west coast where a single blade propeller was used. Pierce describes the theory behind the Everel propeller and comments that the "cub was cruising at an average of ten miles an hour faster than usual" under all conditions[6]. This supported Everel's claim that the propeller could extract more power out of the small engines of the time to push airplanes faster. However, with advances in engine technology, the Everel propeller was overshadowed and never caught on. This was further impacted by the heavy weight which was now



Figure 2-5: Everel propeller mounted on a J-2 Cub aircraft

seen as unnecessary and the price tag which was roughly 10 times that of a similar two bladed propeller.

More recently, Gene Breiner took an interest in the Everel design and installed one on his Cub to determine its performance. Using this airplane as a test platform, it was connected to a scale to determine the thrust produced. However, contrary to Everet's claims that the propeller was able to produce more thrust, it was consistently producing 10% less thrust than a traditional two blade propeller. In addition to this, the propeller has proven to be very temperamental to changes in weather and humidity and requires excessive adjustments to the counterbalance to ensure proper operation. [7]

#### **2.4.2 Single Blade Propeller Development by WHOI**

The idea to utilize a single blade propeller for UUVs was proposed by Jeffrey Kaeli and Frederick Jaffre at WHOI. Unlike the Everel propeller designed to increase thrust, the use of single blade propeller was intended to increase efficiency of the propeller and also provide a means of maneuvering the UUV. With computing power available to modern UUVs such as the REMUS on which the concept was tested, the UUV has the capability to modulate the speed of the propeller throughout the rotation. With

a varying propeller speed, the overall propulsive force depends on the average angular speed of the propeller. However, because the speed changes throughout the rotation, the distribution of the force is no longer uniform. This results in a moment which serves to steer the UUV. The concept is similar to how a quadcopter uses multiple rotors to enable powering as well as steering. However, rather than increasing the speed of rotors on one side of the quadcopter, the same propeller is sped up through part of a rotation. Figure 2-6 shows how the varying speed of rotation leads to an overall thrust and steering force.

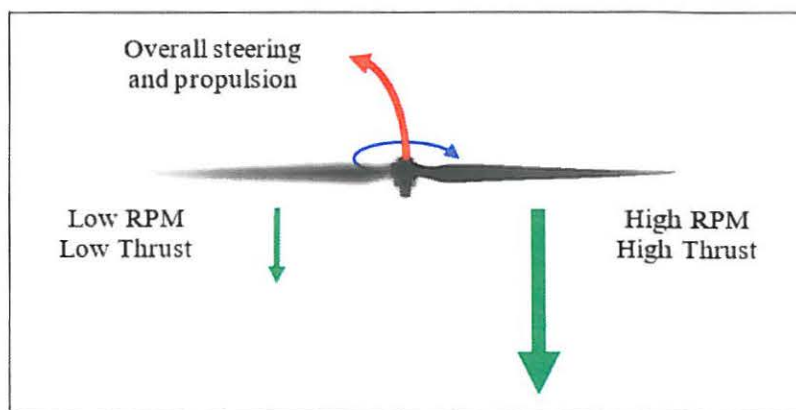


Figure 2-6: Single blade propeller functional concept

## 2.5 Summary

As the Navy continues the push for more capable unmanned vehicles, there is a need for new technologies which will enable new missions. If feasible, a single blade propeller can be a technology that fills a capability gap which currently exists for smaller UUVs. It can offer an innovative way of propelling and steering a UUV that operates on different principles, vectored thrust instead of lift. This can have implications for everything from the performance of the UUV to its integration on a host platform by providing the maneuverability of a multi-rotor UUV with the form of a cylindrical UUV.

# Chapter 3

## Stakeholder analysis

### 3.1 Distributed Lethality Concept and the Role of UUVs

After the end of the cold war, the US Navy was able to operate relatively freely for many years without any near peer competitors. However, in recent years this trend has been changing and new tactics have begun to evolve to account for new technologies and threats. For the surface fleet, this has meant a shift from the traditional surface action groups (SAG) which were centered around the high value unit (HVU). This construct allowed for the safe operation of the HVU which could then support other operations, such as air support for land forces. When operating against a near peer competitor, and the possibility of operating in an anti-access/anti-denial (A2AD) environment means that the traditional SAG may not be able to position where it has historically been able to accomplish its mission. From a white paper on distributed lethality, it is defined as “the condition gained by increasing the offensive power of individual components of the surface force and then employing them in dispersed offensive formations known as hunter-killer SAGs.”[6] The idea is to use several smaller yet capable hunter-killer SAGs as opposed to fewer, smaller high impact SAGs concentrated around a capital ship. The smaller hunter-killer SAGs will be comprised of a greater mix of ship capabilities that balances overall capability with cost. With

many hunter-killer SAGs the enemy can no longer just focus on the traditional HVUs and “every warship is a potential sensor or shooter in the shared effort, but the ability of enemies to detect, track and target U.S. naval forces is greatly complicated.” [2]

While the distributed lethality concept was developed with current surface assets in mind, the same principle has created a push to further integration of unmanned vehicles in the Navy. By adding UUVs to the existing ship and submarine mix, the capability of those units is extended and allow for individual units to accomplish operations that would otherwise not be possible. In 2000, the Navy published a road map which has subsequently been updated to give guidance on how UUVs will be implemented in the future. The aim was to “define UUV capabilities [that] establish levels of performance for each capability, and to recommend the appropriate vehicle classes and technology investments required to efficiently achieve these recommended capabilities.” [4] This was useful to understand what aspects of UUV design were important to the Navy and where this technology would fit in to provide an alternate and possibly better suited solution. Figure 3-1 shows the vision for how UUVs would be employed in the future for different warfare areas.

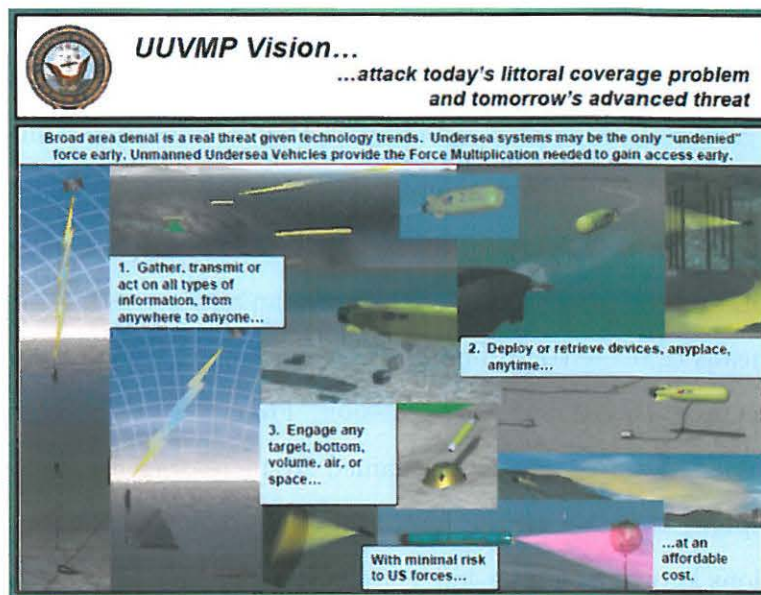


Figure 3-1: UUV Master plan vision for future warfare areas [4]

### 3.2 Requirements for future UUVs

The initial CONOPS from the UUV Master Plan, is further distilled into nine mission pillars that are outlined for UUVs to accomplish. These include Intelligence, Surveillance, and Reconnaissance (ISR) and Information Operations (IO), Mine Countermeasures (MCM), Anti-Submarine Warfare (ASW), Inspection / Identification, Oceanography, Communication / Navigation Network Nodes (CN3), Payload Delivery, and Time Critical Strike.[4] Based on the breadth of missions, the road map specifies attributes that would be required for each mission which allowed me to derive the overall needs for future UUVs. Each of the mission pillars high level specifications are shown in Table 3.1.

	Radius of operation	On station time	Speed	Size
	NM	hours	knots	
ISR	50-150	100-300	3-7	Medium-Large
ID	1	>12	3	Small
MCM		Similar to ID		
ASW	10-100	10-400	3-12	Large
Oceanography	-	10-12	-	Small-Medium
CN3	10-250	72	2-5	Small
Delivery	100	>2000	2-5	Large
Strike	100	>100	2-5	Large

Table 3.1: Mission pillars for UUVs [4]

While the UUV masterplan does set out other specifications for some of the mission pillars, I chose these attributes to highlight because they were common to multiple mission pillars and most relevant to the propulsion aspect of the UUV. The largest takeaways from this study which are applicable to this thesis was the focus on endurance and the low end of speed requirements under which the UUV would be required to operate.

The other two major applicable takeaways for requirements from the UUV masterplan is the need for deployability and maneuverability for certain missions. The UUVs envisioned would come in four different sizes. The first is size to be portable by a single person weighing no more than 100 lbs. The light weight class will be approximately 13” in diameter and weigh up to 500 lbs. The heavy weight vehicle

class will be up to 21" in diameter and weight up to 3000 lbs. The final class is the large vehicle which will be over 20,000 lbs. The first three classes of UUVs must be compatible with current submarine and surface launch capabilities while the large vehicle must be compatible with existing surface capabilities and some submarine capabilities. This creates an envelope and maximum diameter that the UUV must conform to in order to ensure it can be stored and deployed. When considering cylindrical UUVs such as those shown in Figure 2-2, this means that the extent of the fins or any other appendages must be inside the max diameter. The need for maneuverability applies in all cases, however it is specifically highlighted for mission like ID and MCM. In cases like these the UUV must be able to avoid closely spaced obstacles as well as maintain its orientation while operating at low speeds. The UUV masterplan calls out the ID mission as requiring "a higher degree of control than is often found in more conventional cylindrical UUVs." [4] This shows the perceived incompatibility with traditional slender UUVs and precision maneuvering.

Based on these requirements, I was able to determine the needs that could be addressed by implementing an asymmetrical propeller for UUVs:

1. The UUV must be capable of the highest speed required for its mission - Thrust and drag requirements
2. The UUV must be compatible with all current modes of transportation and delivery - Form factor requirements
3. The UUV must be maneuverable in all portions of the mission speed range - Control authority requirements
4. The UUV should maximize its on station time through an efficient power usage - Propulsive efficiency requirements
5. The UUV should be as simple as possible - Robustness and survivability

### 3.3 Decomposition of a UUV

As with many mechanical systems, each architectural decision on a UUV balances improved performance in one aspect with an acceptable performance decrement in an alternate aspect. To characterize some of these trade offs I used a decomposition of the formal elements of a UUV to see how they related to different aspects of the UUV mission. I chose to focus on four aspects of the UUV performance. The straight forward attributes included endurance, speed, and host vehicle which address needs 1-3 from the requirements in Section 3.2. The final aspect is the suitability for specific missions. This takes into account things like the maneuverability of the UUV, the payload capability, form of the UUV, and power available for the payload as compared to what is required for other systems. Figure 3-2 shows the differences in decomposition for the traditional and proposed propulsion and control methods for UUVs.

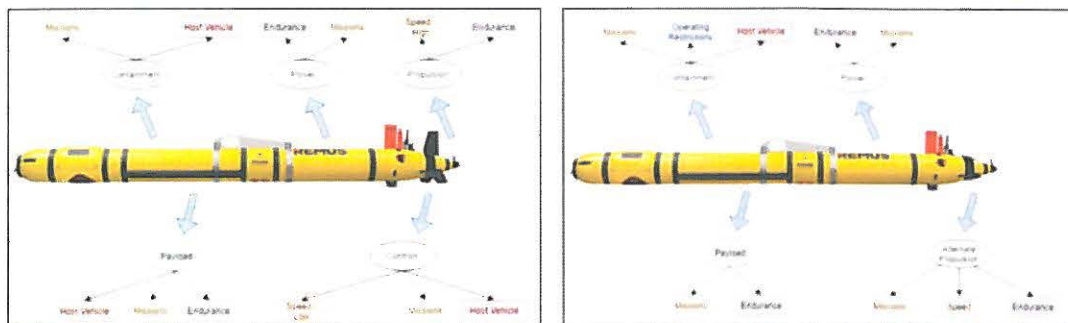


Figure 3-2: Formal decomposition of UUVs with control surfaces (left) and asymmetric propeller (right)

This method of decomposing the physical components of the UUV and connecting them to specific performance attributes allowed me to evaluate how the new propulsion method would impact the UUV operations.

The two major differences in Figure 3-3 come in the host vehicle compatibility and speed performance attributes. This comes from the fact that with the alternate propulsion, there is no longer a need for additional control surfaces on the UUV. Additionally, the speed is dependent on only the alternate propulsion rather than

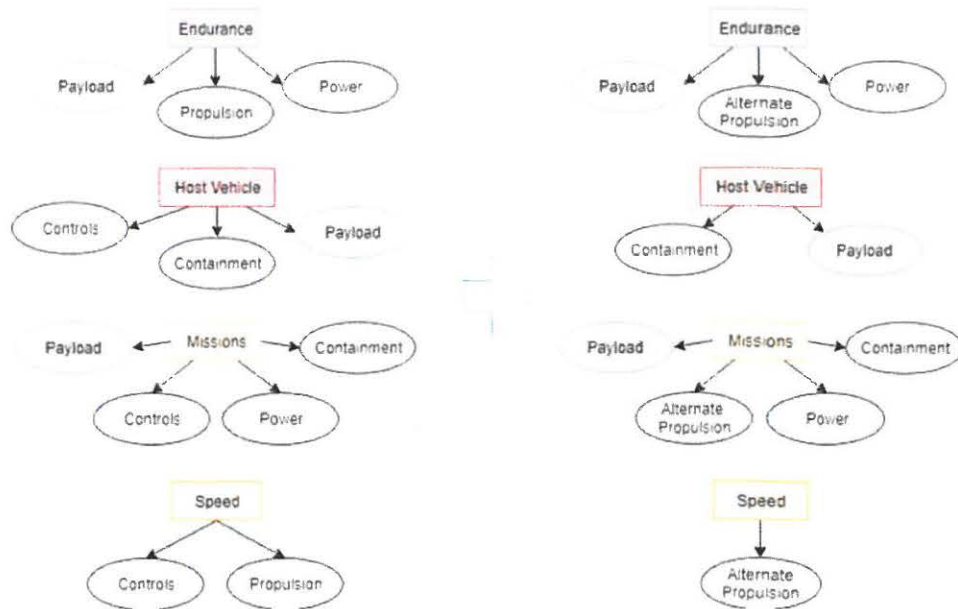


Figure 3-3: Mapping of performance attributes to UUV design

competing interest for the propeller and control surfaces. Finally, the mission and endurance are now dependent on the alternate propulsion vice control method and propulsion. So any improvement in the efficiency of the propeller or maneuverability would yield an improvement in these performance attributes.

### 3.4 Use Case for Asymmetric Propeller

#### 3.4.1 Benefits

The benefit from using the asymmetric propeller could come from three aspects of its performance. The first is the possibility for the increased maneuverability. The maneuverability of the UUV can be characterized by the control authority, which is the size of the force the steering mechanism is able to create to turn the UUV. When a control surface is used, the force generated is due to the lift created by a foil at an angle of attack as seen in Figure 3-4. The magnitude of the lift is a function of the

foil shape, the angle of attack, and the square of the velocity of the flow over the foil. Most of these factors are limited by design, however speed will vary throughout the operation and a change in speed to 25% of the original speed can result roughly 95% decrease in the steering force. [3] In a UUV where the top speed is relatively low, this becomes a bigger concern. Additionally, there is a stall speed where the rudder is no longer effective. On surface ships, this can be mitigated by placing the control surface behind the propeller so that even at low speeds the propeller is creating flow over the rudder. With the rudder ahead of the propeller as in most UUVs, the flow is significantly diminished.

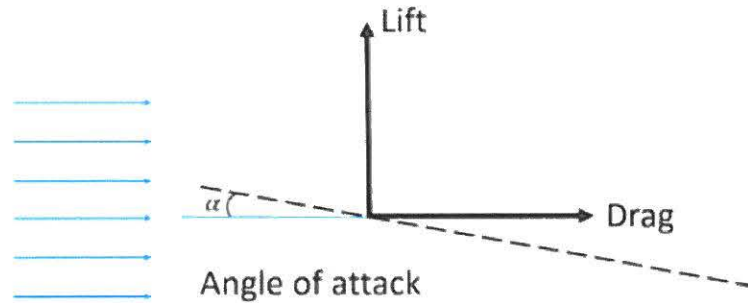


Figure 3-4: Mode of operation for control surfaces

Using the asymmetric propeller allows for the amount of thrust generated throughout the rotation of the propeller to be varied which functions similar to vectored thrust for an airplane. As a result, the UUV is no longer dependent on forward motion for control authority and depends more on the rotation of the propeller. The result should be a more uniform control authority over the speed range of the UUV. Figure 3-5 shows a notional comparison between the control authority for a standard rudder configuration and a propeller steered UUV. For this comparison, I assumed the propeller steered UUV had a top speed of 4 knots which was used to determine the propeller thrust and thus the steering force. For the rudder controlled UUV I assumed the same top speed and two control surfaces which were 30  $cm^2$  each. While this calculation does not take into account all the factors for either steering case,

it shows the tradeoff leading to each configuration having a better performance in one area. The calculations and formulas used for this approximation are included in Appendix A. For this UUV, if most of the mission required operation in the top half of its speed range, the rudder performs roughly equal if not substantially better. Conversely, an UUV operating in the lower half of the speed range using the propeller for control authority is the superior architecture.

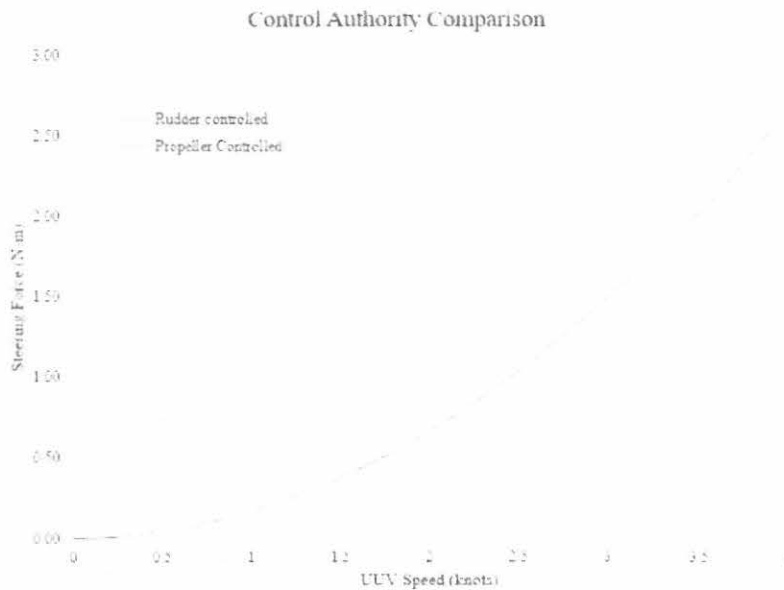


Figure 3-5: Control authority comparison

The second aspect where a single blade asymmetric propeller could outperform a multi-blade propeller is in propulsive efficiency. This would come from two aspects, the reduced drag from control surfaces and the performance of the propeller. As shown in Figure 3-4, whenever a control surface is used, it generates a drag force as well as the lift force. There is an additional baseline drag due to the skin friction on the control surfaces, however this force is relatively small. By removing the need for control surfaces, the UUV will have lower drag both when it is and is not maneuvering.

In addition to this, having fewer blades could result in a higher efficiency for the propeller. In the past, tests have been run with a standardized propeller design and

varying parameters systematically. One expansive standardized series is the Wageningen B-Series propeller which was originally tested by the Netherland's Ship Model Basin. By varying propeller parameters, including number of blades and other propeller geometry, designers could see general trends in propeller performance. While no testing has been performed to date to compare the performance of a single bladed propeller, it would follow the general trend shows in Figure 3-6 that reducing the number of blades leads to higher efficiency. In this diagram the advance ratio represents an operating condition which is dependent on the velocity of the UUV and the rpm of the propeller. As shown in Figure 3-3, the endurance is dependent on the size of the battery, the power required for propulsion, and the power required for the payload. Reducing the power required for propulsion allows for a larger or more power hungry payload for the same size UUV.

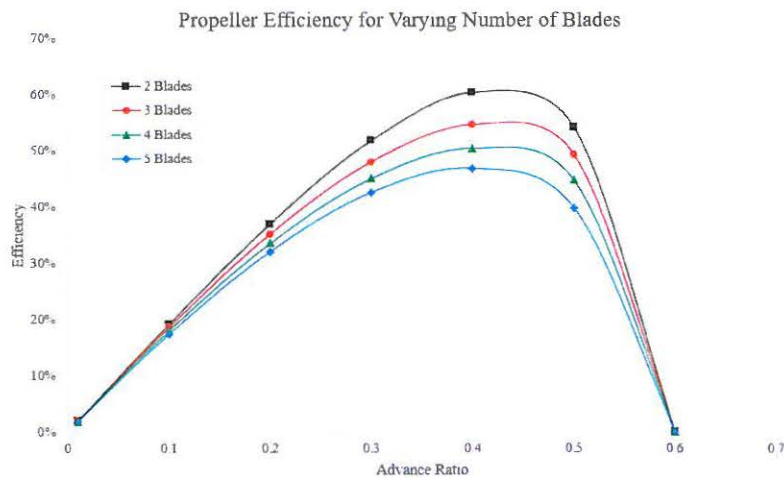


Figure 3-6: B Series propeller efficiency

The final benefit that could be obtained from the asymmetric propeller is the reduced mechanical complexity of the UUV. The control surfaces need to be movable which results in additional penetrations to the containment that must be maintained waterproof as well as an additional mechanical system. By removing this, there would be one fewer mechanical failure mode for the UUV.

### 3.4.2 Trade Offs

While there are several possible benefits to a single blade propeller, each also has a cost associated with it. While the single bladed propeller is more efficient overall than a propeller with similar geometry and more blades, it may not be feasible for all missions. As a result of using the propeller for maneuvering, it is no longer operating at a constant speed. Where a traditional configuration would be able to maintain its higher speed and use the fins to steer the UUV, the single blade variant would need to employ a lower speed through part of the rotation and thus sacrifice speed. The other loss in speed would come from the operating characteristics of the propeller. Another aspect explored in the B-series propeller testing is the thrust generated by each propeller as seen in Figure 4-3. The thrust coefficient,  $K_t$  which is proportional to the thrust generated by the propeller, decreases with the number of blades. This is because a propeller generates its propulsive force by creating lift with the blades. For a propeller with fewer blades, the amount of lift decreases and leads to lower overall thrust.

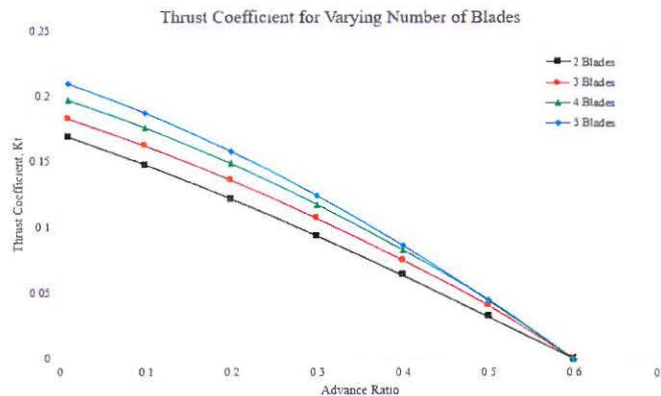


Figure 3-7: B-series propeller thrust

Finally, while the asymmetric propeller reduced the mechanical complexity of the UUV, it does introduce the potential for vibration issues. This can be reduced by providing a counterbalance for the propeller, but the fact that the thrust force developed by the propeller is not balanced axially means there will always be some

induced vibrations that need to be accounted for.

### 3.4.3 Summary

The tradeoffs described in sections 3.4.1 and 3.4.2 can be consolidated into six broad performance attributes, maneuverability, speed, endurance, mechanical complexity, electrical complexity, and robustness. Because the cylindrical UUV is largely the standard form for Navy uses, I used that as the baseline when considering the multiple thruster and single blade alternate architectures. Table 3.2 uses a Likert-type scale to show the relative performance of the alternate architectures as compared to a baseline cylindrical UUV. A 0 indicates performance similar to that of a cylindrical UUV while a 1 is somewhat different and a 2 is significantly different. A positive number indicates more desirable performance and negative indicates less desirable. Overall, the single blade propeller provides a lesser degree of the positive aspects of a multiple thruster UUV without the same operational restrictions.

	Cylindrical UUV	Multiple Thruster UUV	Single Blade UUV
Maneuverability	0	-2	+1
Speed	0	-2	0
Endurance	0	-2	+1
Mechanical Complexity	0	0	+1
Electrical Complexity	0	0	-1
Compatibility	0	-2	0

Table 3.2: Performance comparison against traditional cylindrical UUV

THIS PAGE INTENTIONALLY LEFT BLANK

# Chapter 4

## Test Program

### 4.1 Overview

Before attempting to gain an understanding of abnormal operating conditions for the single bladed propeller, it was necessary to understand its baseline performance. This included the key performance parameters such as the thrust generated by the propeller and its efficiency in doing so. Additionally, traditional propeller testing evaluates the torque required to operate a propeller in a given operating regime. To accomplish this, I used a method known as open water propeller testing. This method requires a tow tank with a powered carriage that can tow the test rig.

After this was completed, I moved to a side by side comparison of the control authority of the single bladed propeller and the and a traditional control surface setup. During this part of the test, a UUV provided by WHOI was instrumented and used to test for the control authority. This configuration was not intended to provide an undisturbed baseline performance like the first phase of testing, but it did provide enough information to understand the relative performance for each configuration.

### 4.2 Open Water Test Theory

While propellers seldom operate in clear flow where there are no disturbances to the oncoming flow, this provides a consistent baseline to compare different propellers. The

International Towing Tank Conference (ITTC) provides guidelines for the setup of open water propeller experiments to ensure consistent results and a uniform method of testing. Figure 4-1 shows the requirements for a test setup to conduct open water propeller testing. In this thesis I focused only on non-duct propellers, so the requirements for the test setup included only a carriage, propeller, and environmental conditions. The carriage and environmental conditions were set by the lab available. The testing was conducted in the Parsons Laboratory at MIT. The facility includes a 100 x 8 x 4ft tow tank with a carriage capable of speeds up to 2m/s. As a result, the remaining test rig had to be designed to be compatible with the existing test infrastructure.

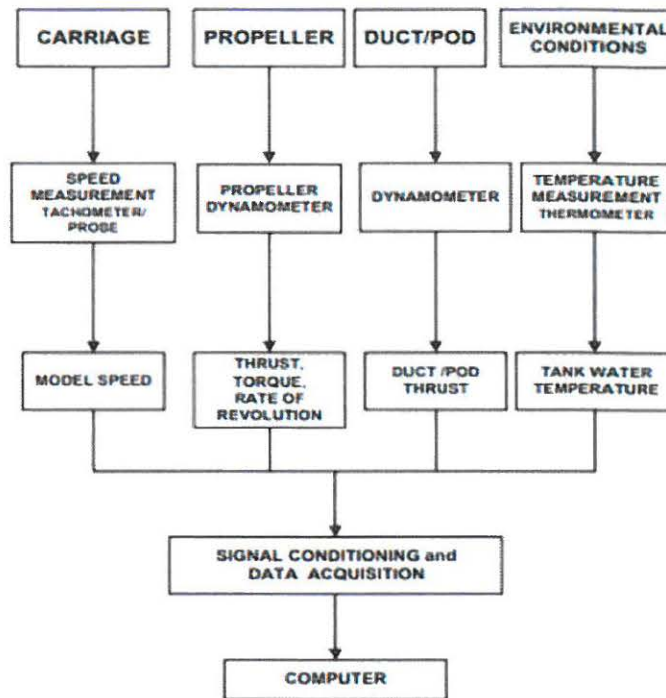


Figure 4-1: ITTC test setup overview [1]

Additional requirements for the configuration are also provided in the ITTC guidelines for open water propeller testing. A sample test rig for open water propeller testing, which is referred to as a propeller boat, is shown in Figure 4-2. This testing is designed to allow the propeller to operate in homogeneous flow and removes the

interaction between the object being propelled and the propeller. To accomplish this, the propeller is mounted on a rigid shaft that is driven ahead of the propeller boat. Inside the propeller boat, the shaft torque, rpm, and axial thrust are measured in order to determine the operating characteristics of the propeller.

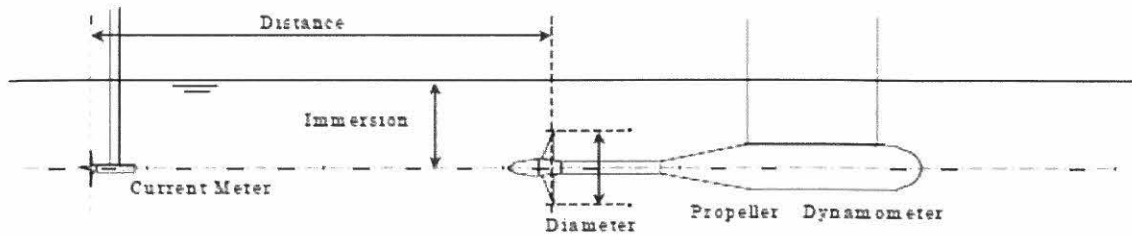


Figure 4-2: Open water propeller test rig setup [1]

As well as guidelines for the test setup, ITTC also provides parameters for the propeller fairing used for testing. Figure 4-3 shows the dimensions for the nosecone and tailcone fairings. These dimensions ensure uniform and clean flow into the propeller and minimize adverse effects from the shaft.

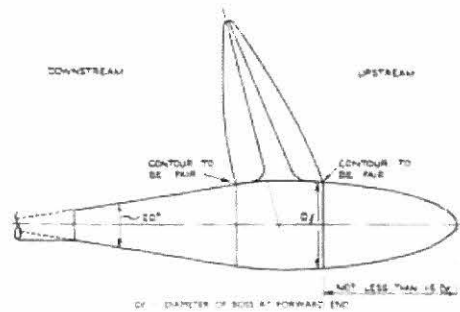


Figure 4-3: Propeller fairing recommendations from ITTC [1]

The propeller is then tested along a variety of combinations of carriage speeds and shaft rpm. This allows for testing under different loading conditions. Unlike a car tire which uses friction to propel a car, a propeller can have a substantial amount of slip because it is using lift to generate the propulsive force. As a result, a propeller

spinning at a given speed can be operating at a variety of velocities of advance. For the purposes of testing, the combinations of propeller speeds and advance velocities are combined into a non-dimensional coefficient called the advance ratio which is shown in Equation 4.1.

$$J = \frac{V_a}{nD} \quad (4.1)$$

During an open water propeller test, the propeller is tested over a variety of advance ratios to determine its operating characteristics under normal conditions. The thrust developed by the propeller and the torque required to spin the propeller are recorded at each advance ratio and used to calculate non-dimensional coefficients for thrust ( $K_t$ ) and torque ( $K_q$ ) which are shown in Equations 4.2 and 4.3. In these equations,  $\rho$  is the water density,  $n$  is the propeller rpm, and  $D$  is the propeller diameter. Based on the thrust and torque of the propeller, the open water efficiency,  $\eta_o$ , is determined using Equation 4.4. This is the efficiency of the propeller when it is operating without any flow disturbances. This number will vary from the expected performance of the propeller during use on a ship. However, these coefficients allow for easy comparison of different propellers under ideal conditions. Additionally, using the coefficients, the results can be scaled such that a smaller model propeller can be used to determine the characteristics of a full size ship propeller. For the purposes of this thesis, I was not interested on scaling results from my testing since the result of concern was a comparison of performance.

$$K_t = \frac{T}{\rho n^2 D^4} \quad (4.2)$$

$$K_q = \frac{Q}{\rho n^2 D^5} \quad (4.3)$$

$$\eta_o = \frac{J K_t}{2\pi K_q} \quad (4.4)$$

The three parameters are normally displayed graphically, similar to the results

for a standardized propeller series shown in Figure 4-4. For a screw type propeller, there are several typical characteristics to look for. The first is the decrease in thrust as the propeller operates with less slip at higher advance ratios. This is because as the advance velocity increases, the angle of attack of the blades decreases. At an advance ratio slightly higher than the pitch of the propeller, the thrust will be zero representing the speed at which the angle of attack is insufficient for the propeller blades to generate lift. This is a factor of the propeller geometry and will occur at the same advance ratio for any propeller with the same blade pitch.

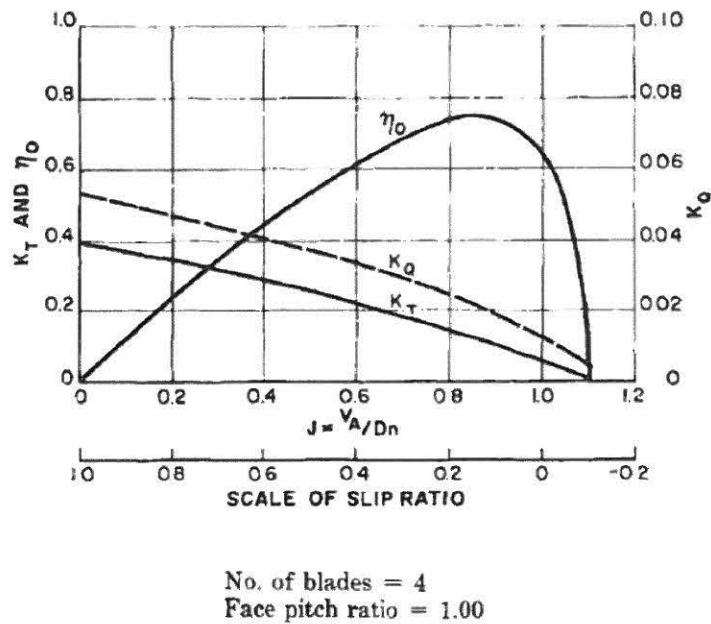


Figure 4-4: Open water propeller test sample results

### 4.3 Propeller Boat Design

Before beginning the design and construction of the propeller boat which would be used for testing, I evaluated the resources available at the MIT tow tank and for the project to determine the limitation on the project. The main limitation from the tank was the physical connection requirements. Additionally, there was limited

funding available for constructing the propeller boat which meant that being able to reuse any material was ideal. With this I evaluated my options to create a test setup compatible with existing infrastructure while minimizing costs.

### 4.3.1 Propeller Boat Tradespace

During the initial phase of the propeller boat design, I considered the most important architectural considerations which could be modified for my design. I started with the general configuration that I needed and was able to decompose that into the architectural decision I had in my design. For this I consulted two institutions that are currently using propeller boats which were designed for similarly sized tanks. The United States Naval Academy recently built a propeller boat which was intended for testing water turbine blade designs and run in their 100 ft tank. Webb Institute had a senior thesis which detailed the process designing and constructing of their propeller boat which is used for testing propellers in the 93 ft tank located on campus. These two designs are vastly different and gave me a spectrum of design options that I could look into and possible solutions for my design. After studying these propeller boats I began by determining the key architectural decisions.

The propeller boat can be decomposed into three major components, the structure, the driving mechanism, and the sensors. Within the driving mechanism the major design choices were the type of motor used type of connection to the propeller shaft. The structure similarly can be split into the material and type of enclosure used. In each case, an enclosure for the main structure would be necessary, however, it could be used just as a fairing to reduce resistance force on the carriage or may also be required for protecting the internal components. Table 4.1 shows the architectural decisions as well as the evaluated solutions.

The first decision I made was the material used for the structure. While steel would have provided a stronger and more rigid structure, the abundance of T-slotted aluminum and the ability to easily integrate it into the current tank infrastructure made it a better option. Additionally, the propeller boat will be stored in a humid environment and is required to operate submerged in water. This meant that any

Test Rig Design Space				
Motor Selection	DC Stepper Motor	AC Motor		
Drive type	Right angle gears	Direct	Chain	Belt
Sensor	Combined (IP68)	Commbined (non-IP68)	Separate (IP68)	Separate (non-IP68)
Structure	Fiberglass	Aluminium Steel		
Enclosure	Watertight	Non-Watertight		

Table 4.1: Test Rig Design Tradespace

steel used would have to either be stainless steel which is expensive, or have periodic maintenance performed to prevent corrosion. From the remaining decisions I created several possible solutions that were evaluated for my test setup. The five main alternatives evaluated are shown in Figure 4-5. These options combined the remaining architecture decisions from Table 4.1 and evaluated the benefits of each. Once the options were created and evaluated I determined which architecture had cons which could most easily be overcome. The combined waterproof sensor would have provided the most reliable data with the simplest construction requirements because it could be placed in line with the propeller and with minimal friction between the sensor and the propeller. However, due to the small number of applications for this sensor, there are not extensive options for purchasing one which results in a higher cost. The other options required separating the measurements into thrust and torque which allowed for them to be placed at different location along the drivetrain. This meant that only the thrust sensor if any would require waterproofing. The other main difference between the remaining options is the drivetrain. The advantage of the bevel gears was that if properly designed, they would be a smoother option as compared to the longer chain that was required as well as providing a convenient point for measuring thrust.

The final design selected was alternative 1 which uses a chain drive to power the propeller shaft with a non-waterproof sensor located in the upper shaft and a waterproof sensor used to measure the thrust produced by the propeller. This configuration removed the need for a waterproof housing while reducing the cost of the required

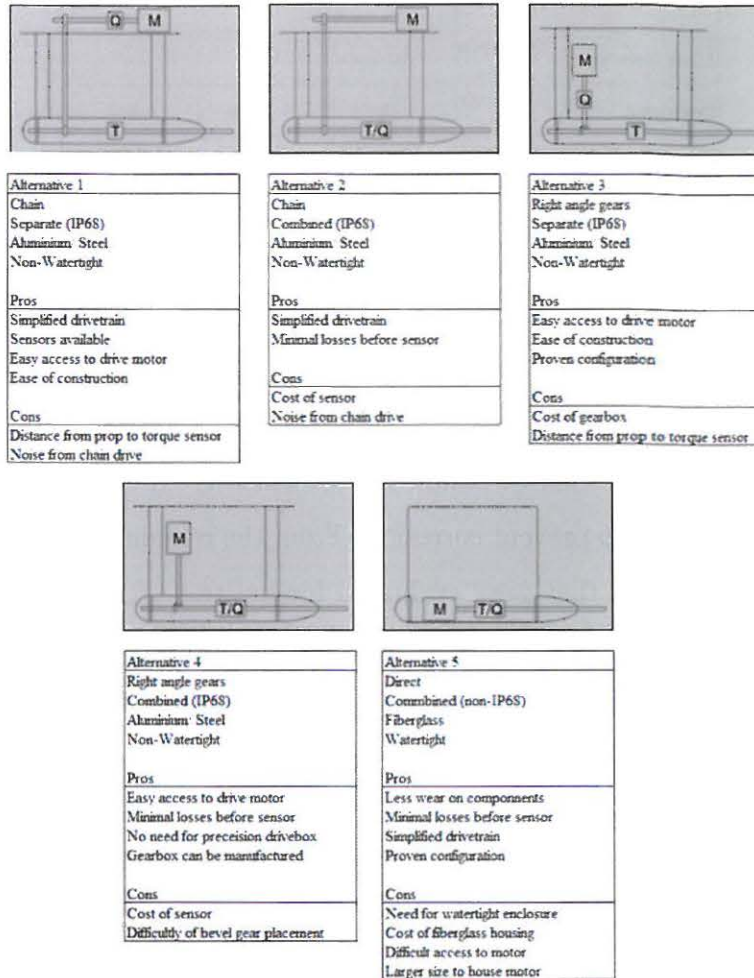


Figure 4-5: Possible test setup architectures

instrumentation as compared to the combined sensor. For all cases, a new torque sensor would be required, however, waterproof force sensors for the thrust were available at MIT for use in this project. The decision to go with a chain drive over the bevel gears was made based on the complexity of a precision gearbox that was required. By using the chain drive, I was able to ensure that all of the manufacturing of the propeller boat could be done using the student shops at MIT. The final design for the propeller boat can be seen in Figure 4-6.

This design balanced the ability to obtain reliable results with ease of manufacturing and cost. While I understood the data would not be as clean as a direct

measurement of torque and thrust closer to the propeller on the main shaft, I believed that this could be overcome through the post processing of the data.

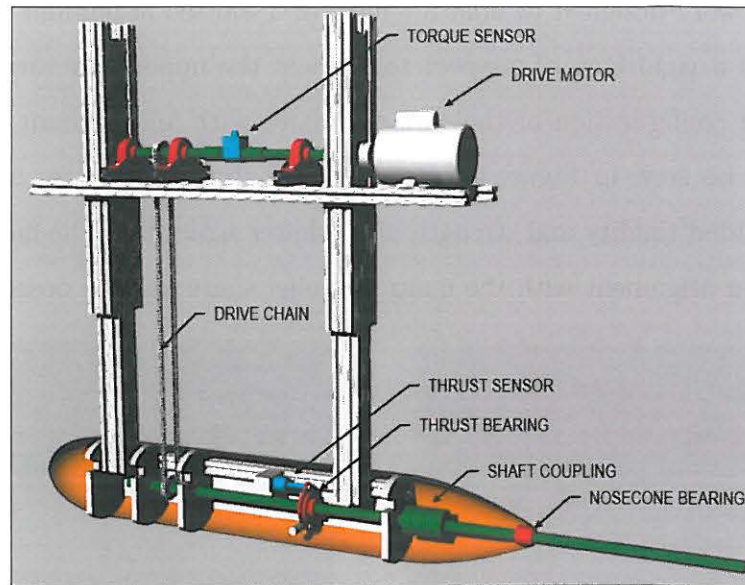


Figure 4-6: Rendering of propeller boat design

## 4.4 Propeller Boat Detail Design and Construction

The detailed design of the propeller boat can be broken down into two parts, the upper structure which supported the drive motor and torque sensor, and the lower structure with the propeller shaft and the thrust sensor. The majority of the design was utilized T-slotted aluminum. This allowed for quick and easy construction and modification to the design as needed. The T-slot system and numerous standardized connectors allowed for many connection points and easy adjustments to the components in the upper structure as well as its connection to the lower structure. For the lower structure I decided to machine the components out of aluminum stock which allowed for more precise construction than the T-slotted system. Unlike the upper structure which could accept larger amounts of misalignment and function properly, the lower structure required a much longer continuous shaft that could have binding if not carefully aligned.

To ensure proper alignments, I used 4 brackets that were machined in tandem which to house the bearing and be the guide for the rest of the structure. The support plates were designed to hold a length of T-slotted aluminum on either side which provided a rigid base of support to connect the upper structure to the lower structure. The configuration of the support plates with and without the T-slotted aluminum can be seen in Figure 4-7. Additional aluminum plates were added to each side for added rigidity and strength of the lower structure. The final component requiring proper alignment with the main propeller shaft was the nosecone.

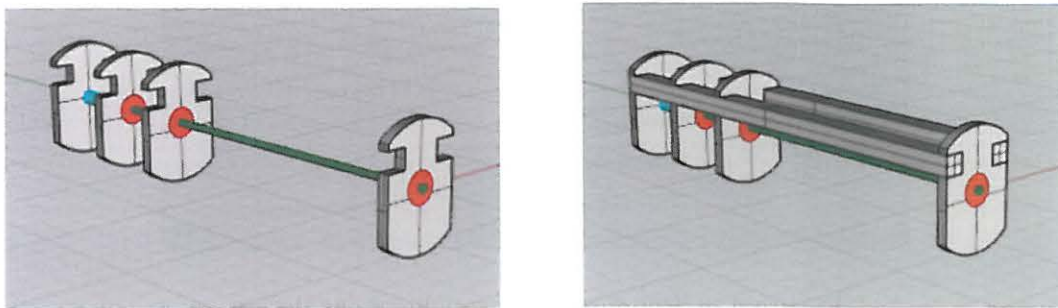


Figure 4-7: Propeller shaft with support plates shown with and without T-slotted aluminum

While the nosecone was primarily required as a fairing to reduce the towing forces on the carriage and the upstream effect of the flow, it did need to provide support to the shaft. The last bearing was in the front support plate and the propeller shaft extended roughly 60cm beyond this point. Because of the high speed rotating load at the end of the shaft, even a small imperfection in the shaft or propeller would cause excessive vibration without support closer to the propeller. To reduce the risk of this, I machine the nosecone out of delrin. Delrin was selected because it is rigid enough to provide the support needed but lighter than other alternatives. Initially, I had planned to machine the delrin to provide a tight fit around the propeller shaft, however, due to challenges of machining such a large piece of delrin I decided to use a sleeve bearing in the end of the nosecone instead to provide a more precise point of support. The final lower structure with the nosecone installed can be seen in Figure 4-8.



Figure 4-8: Final lower structure with nosecone

Once the main components of the lower structure were completed, I began assembling the upper structure. For this application I was able to use self-aligning bearing mounted to the T-slotted aluminum to create the upper portion of the drivetrain. I manufactured two collars which were used to connect the driveshaft to either end of the torque sensor. The final upper structure assembly can be seen in Figure 4-9.

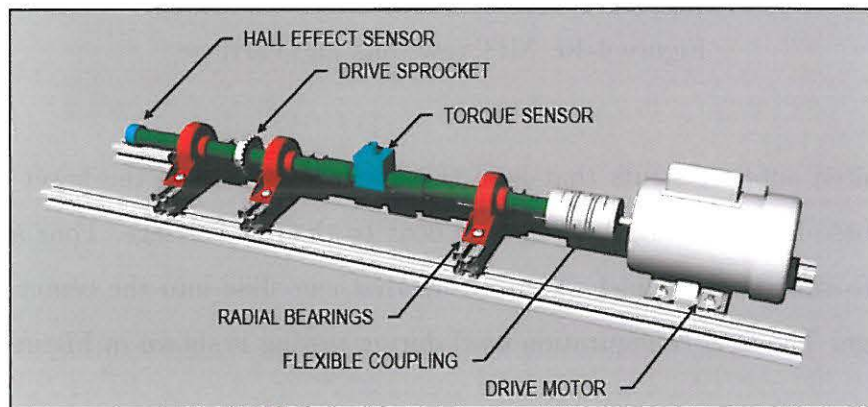


Figure 4-9: Final upper structure configuration

With the upper and lower portions constructed, I was able to connect them using the T-slotted aluminum. The struts used for connecting the upper structure to the lower structure was also faired to reduce the drag and hydrodynamic effects of the propeller boat. Additionally, the rear strut fairing needed to accommodate the chain

connecting the two shafts to shield it from the flow as the propeller boat was towed. This was to prevent any drag on the chain from being imparted onto the propeller shaft and being sensed by the thrust sensor. The final consideration was attaching the propeller boat to the towing carriage in a way that allowed for it to be easily installed and removed. This was facilitated by the tow carriage being configured with the same T-slotted aluminum structure as the propeller boat. Figure 4-10 shows the configuration of the MIT tow tank as well as the tow carriage. The aluminum structure rides on a central beam that supports the weight and propels the carriage down along the tank.



Figure 4-10: MIT tow tank and carriage

The faired support struts that held the upper structure to the lower structure were the base for mounting the propeller boat to the tow carriage. Four arms were attached to this portion which extended up that can slide into the center beam on the carriage. The final configuration used during testing is shown in Figure 4-11.

#### 4.4.1 Sensor Selection and Placement

One of the main challenges during the design and construction of the propeller boat was obtaining consistent and correct reading from the thrust sensor. When starting the project, I had sourced a Kistler gauge, which is a piezo electric sensor that allows for very precise measurements and is able to function underwater for extended periods of time. I had used this type of sensor on previous projects measuring drag

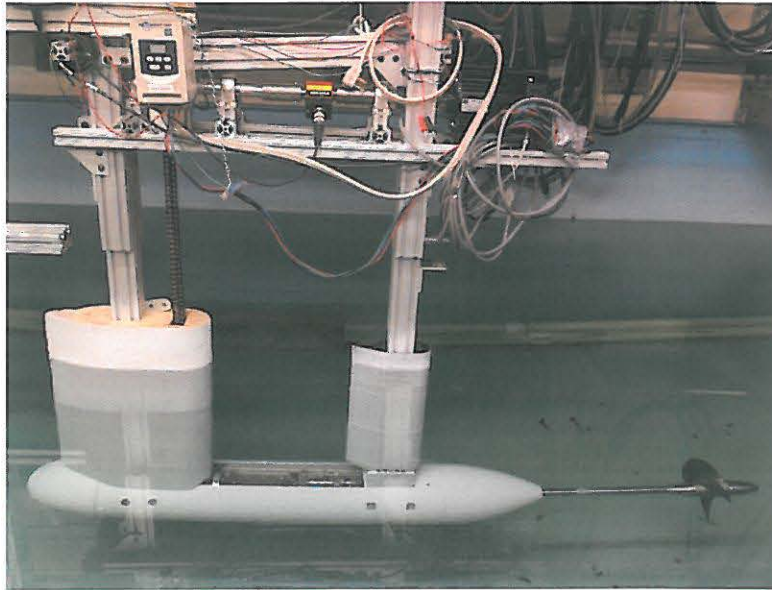


Figure 4-11: Final propeller boat configuration mounted to tow carriage

of underwater bodies which would have been similar to the steady state forces I was trying to measure during the test runs. However, during testing I was unable to get consistent performance from the Kistler gages available. Figure 4-12 shows the information path for data collection with a Kistler gage. The Kistler gage works by using a crystal to generate a charge based on the deflection of a crystal. This charge is sensed by an amplifier which generates a voltage based on the integration of the charge over time and outputs the voltage to a data acquisition module (DAQ).

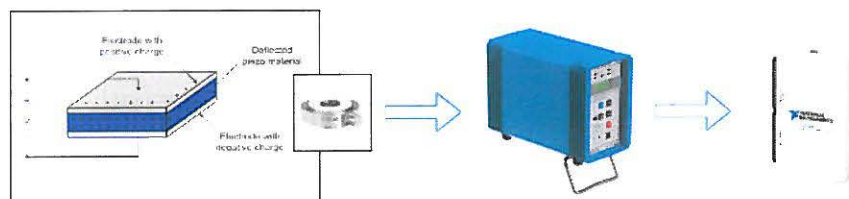


Figure 4-12: Kistler gage information flowpath

A characteristic of piezoelectric sensors, such as Kistler gauges, is that the measurements can drift over time. As a result, the amplifier can be zeroed during testing to provide a standard baseline from which to measure. During initial testing I

performed with the Kistler gauge, the basic functionality seemed to be working as expected. The sensor would register forces and the zeroing function on the amplifier would reset the measurement. However, once the sensor was exposed to water the drift experienced would increase significantly. After the sensor had been immersed in the water for a longer period of time, rather than acclimating it would begin to respond erratically. The same force could register as a positive or negative voltage depending on how many times the amp had been reset.

Based on these issues I decided to abandon using the Kistler gauge and shifted to an AMTI sensor that was available and had been successfully used in a more recent thesis at MIT. The primary difference is that the AMTI sensor was a strain gauge vice a piezoelectric sensor like the Kistler gauge. The information flow for the strain gauge is shown in Figure 4-13. The gauge uses the change in conductivity to sense instead of the deformation of a crystal. An amplifier is used to provide an excitation voltage to the sensor as well as to read the output voltage. The output voltage varies as a force is applied to the sensor changes the conductivity of the strain gauge. Similar to the Kistler gauge, the amplifier outputs the final signal to the DAQ.

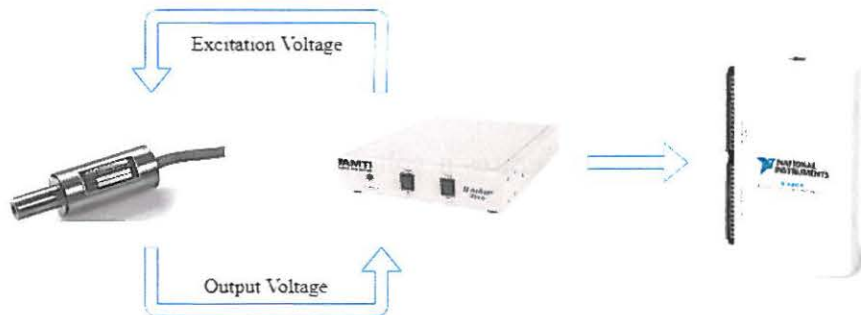


Figure 4-13: AMTI strain gauge information flowpath

Along with issues experienced with the type of sensor, the placement of the sensor was also challenging. The initial design had the force sensor at the end of the shaft between a thrust bearing and the rear support plate. This configuration was chosen because it would provide an easy method for transmitting the force from the propeller directly to the sensor. However, with the sensor in this location, there was an excessive amount of noise in the data recorded as well as a reduced sensitivity in one direction.

This was a result of the type of thrust bearing available for this application. The only bearing available was lower precision which had a large amount of play in the axial direction. While the thrust bearing was completely compressed it read as expected. When the force was in the opposite direction, there was too much friction on the shaft axially to allow the thrust bearing to expand to the other end of its play fully resulting in a smaller deflection of the sensor that was not representative of the force on the shaft. While this was not an issue when the shaft was at the one extreme of the travel range, it was unable to measure forces in both directions as required for propeller testing. The initial and final sensor configurations are shown in Figure 4-14.

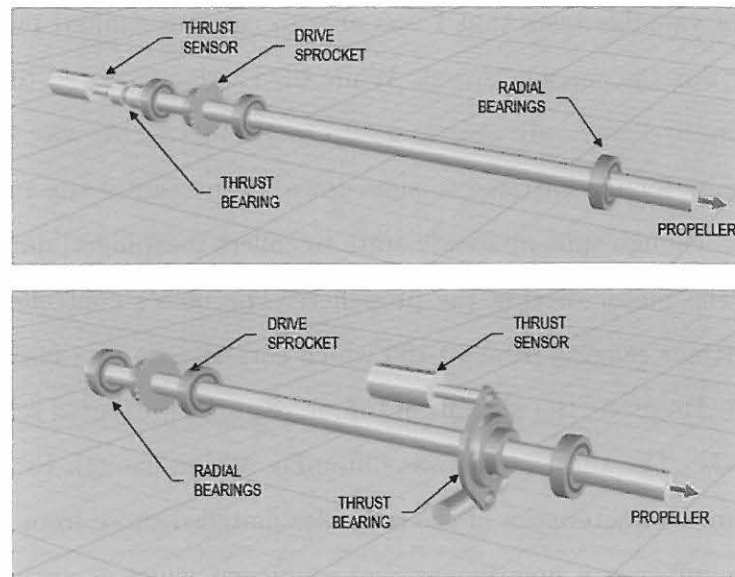


Figure 4-14: Thrust sensor configuration - Initial (top) and Final (bottom)

In the new configuration, I used a radial bearing which was rated to withstand limited axial loads in the range expected by our test propeller. The rated load was below the mid range forces expected during propeller testing. The main concern with this setup was the use of a radial bearing to absorb axial forces. While the loads were within the specification for the bearing, I was able to monitor for potential failure of the bearing during the testing. A sudden change in the torque characteristics could be indicative of a failure of the thrust bearing.

## 4.5 Propeller Boat Validation Process

Prior to beginning testing of the asymmetric propeller proposed in this thesis, I had to validate my propeller boat to ensure that the data being collected was reliable. As a baseline I decided to use a standardized propeller design which had been tested at multiple facilities with ample data for comparison. I was able to obtain a representative propeller from the test facility at Naval Surface Warfare Center at Carderock. This allowed me to run tests on a propeller that had been previously tested and which conformed to the expected results. The propeller used was a 3 bladed propeller with a pitch of 1.070.

The range of valuable tests that I was able to run was limited by three factors. The first factor was the carriage speed. While the carriage is rated to be able to do 2 m/s, operationally I was only able to go up to 1.6 m/s. This was to ensure there was adequate time for the carriage to slow down at the end of the run, but also to ensure there was enough time at steady state to collect meaningful data. The second limitation was the motor driving the propeller. The motor controller was capable of frequency settings ranging from 10-100 which corresponds to a maximum no load speed 1000 rpm. However, the amount of torque required prevented reaching some of the higher speeds. The third factor was obtaining a high enough Reynolds number to ensure the flow characteristics of the propeller matched those from previous tests. The Reynolds number is a non-dimensional coefficient which is an indicator of the type of flow you expect to have on the propeller. The equation for the Reynolds number is shown in Equation 4.5. In this formula,  $C_{0.7R}$  is the distance between the leading and trailing edge of the propeller blade at 70% of the radius from the hub,  $V_a$  is the advance velocity of the propeller,  $D$  is the propeller diameter, and  $\nu$  is the kinematic viscosity of water.

$$Re = \frac{C_{0.7R} \sqrt{V_a^2 + (0.7n\pi D)^2}}{\nu} \quad (4.5)$$

At lower Reynolds numbers the flow along the entire propeller blades is laminar. In this flow regime, the drag on the blades will be inversely proportional to the

Reynolds number. So with a smaller Reynolds number the torque required to spin the propeller could be higher than expected. The aim for the validation tests was to achieve fully turbulent flow in order to match previous tests. This is the normal aim during propeller testing as it allows for the results to be scaled to a full size propeller. In order to achieve fully turbulent flow during testing, the objective is generally to achieve a Reynolds number in excess of  $10^5$ .

## 4.6 Propeller Boat Validation

Based on the limitations discussed earlier I decided to perform test runs at five different frequency settings and 7 different speeds. This was sufficient to cover the majority of the range of operation from low speed operation to the point where the propeller is no longer developing thrust. The test matrix used as well as the Reynolds number for each test can be seen in Table 4.2. While the goal was to have a Reynolds number over  $10^5$  for all test runs, this was not possible at lower carriage speeds due to the drive motor limitations.

	Carriage Speed	Propeller RPM	Reynolds Number
	m/s	rpm	
f = 20	0.25	445	3.7E+04
	0.50	467	5.6E+04
	0.75	490	7.8E+04
	1.00	500	1.0E+05
	1.30	521	1.3E+05
	1.60	538	1.6E+05
	f = 22	0.25	486
0.50		507	5.7E+04
0.75		526	7.8E+04
1.00		544	1.0E+05
1.30		559	1.3E+05
1.60		584	1.6E+05
f = 24		0.25	520
	0.50	547	5.7E+04
	0.75	563	7.9E+04
	1.00	582	1.0E+05
	1.30	599	1.3E+05
	1.60	635	1.6E+05

	Carriage Speed	Propeller RPM	Reynolds Number
	m/s	rpm	
f = 26	0.25	536	3.9E+04
	0.50	560	5.8E+04
	0.75	585	7.9E+04
	1.00	609	1.0E+05
	1.30	637	1.3E+05
	1.60	657	1.6E+05
	f = 28	0.25	570
0.50		585	5.8E+04
0.75		613	7.9E+04
1.00		635	1.0E+05
1.30		662	1.3E+05
1.60		697	1.6E+05

Table 4.2: Validation test matrix

The full results from this testing can be seen in Appendix C along with the expected test results from the original B-series standardized test. Figure 4-15 shows

the test results from the validation testing. In this graph, the expected values for  $K_t$ ,  $K_q$ , and efficiency are plotted in orange. The results from testing are shown using the scatter plot for each frequency used.

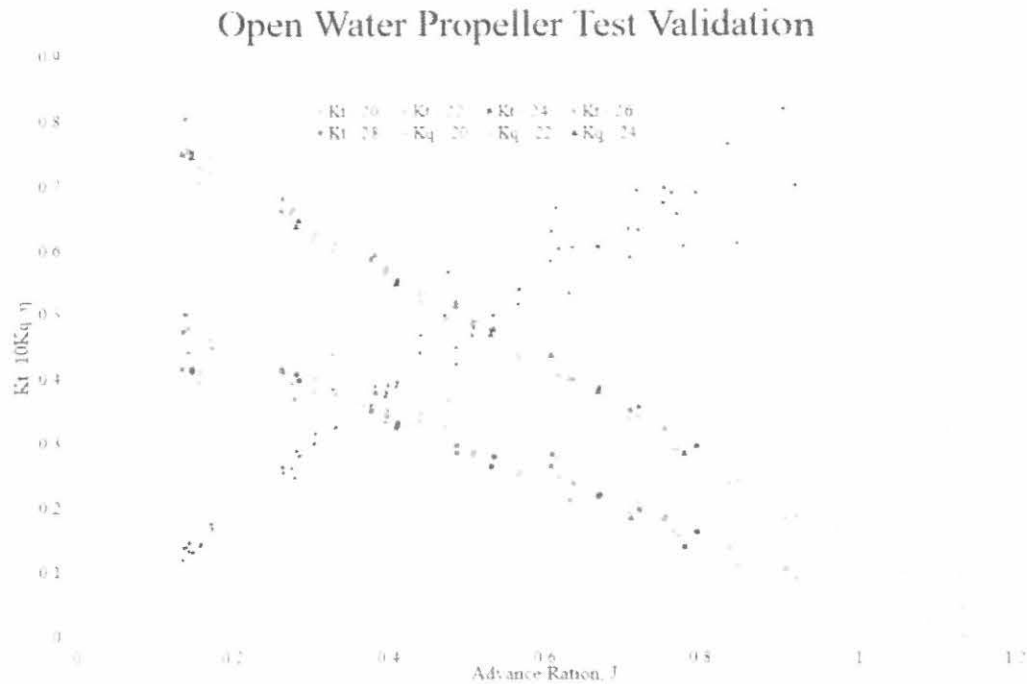


Figure 4-15: Validation test results, expected values shown by orange lines

Overall, the test results I obtained matched closely with those from the previous testing. The maximum error for any point for the thrust coefficient was less than 10% and for the torque coefficient less than 5% with the average values matching almost exactly. The propeller efficiency followed the general trend expected, however there was more scatter at higher advance ratios. This may be due to the fact that both the error in  $K_q$  and  $K_t$  factor into the error in calculated efficiency. By fitting a regression to the data obtained, I was able to compare the results from my tests to the base results. The regression along with the expected results are shown in Figure 4-16. Based on these results I was able to confirm that the propeller boat was operating as expected and could be used for the baseline testing of the asymmetric propeller.

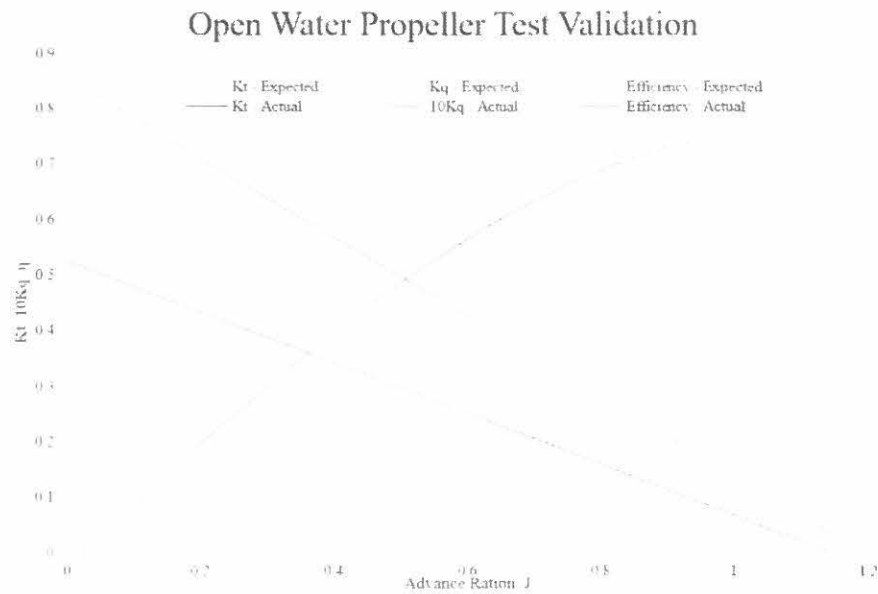


Figure 4-16: Regression for data from validation testing

## 4.7 Single Blade Propeller Propulsive Testing

With the propeller boat functioning and validated, I was able to begin testing the single bladed propeller. Due to the lack of prior testing of a single blade propeller, my goal in this portion of testing was to establish the difference in performance between a single blade propeller and a two blade propeller of the same design. I needed a propeller design that was manufactured in a consistent manner which I would be able to modify to have a two blade and one bladed variant. The propeller selected was an aluminum trolling motor propeller. This propeller was selected because it offered a high degree of uniformity between propellers. Additionally, being made of aluminum made it easy to remove a blade to create a single blade variant. Figure 4-17 shows the original propeller as well as the single blade variant.

The testing for the single bladed propeller followed a similar process to the validation test. From the validation testing I noted that the Reynolds numbers for all of the tests run were adequately high to have sufficiently turbulent flow to obtain good



Figure 4-17: Aluminum propeller used for 1-blade propeller testing

results. This is evident in Table 4.2 because the results for the various propeller RPM does not vary significantly. The correlation was 0.98 for all of the torque data and 0.94 for all of the thrust data across the different propeller speeds. Based on this, I decided to use one propeller RPM for all of the test runs and conduct tests at more speeds between the ones used in the validation testing. The final test matrix can be seen in Table 4.3. The Reynolds numbers for these tests are not as high as the upper end of the previous testing, however they are all within the range used during the validation testing.

Carriage Speed	Propeller RPM	Reynolds Number
m/s	rpm	
0.3	722	4.39E+04
0.5	721	4.79E+04
0.7	726	5.35E+04
0.9	728	6.00E+04
1.1	727	6.73E+04
1.2	734	7.12E+04
1.3	732	7.52E+04

Table 4.3: Single blade propeller test matrix

## 4.8 Control Authority Testing

### 4.8.1 Model Self-Propulsion Tests

The second aspect of the single bladed propeller that I wanted to address in this thesis is the ability to replace the standard propeller and control surface configuration seen single propeller UUVs today. To determine the suitability of the single blade propeller for replacing a rudder I needed to measure the control authority of each to determine the relative effectiveness. For this, I modeled the test program after model self-propulsion tests. The ITTC guidance for a model self-propulsion test is shown in Figure 4-18.

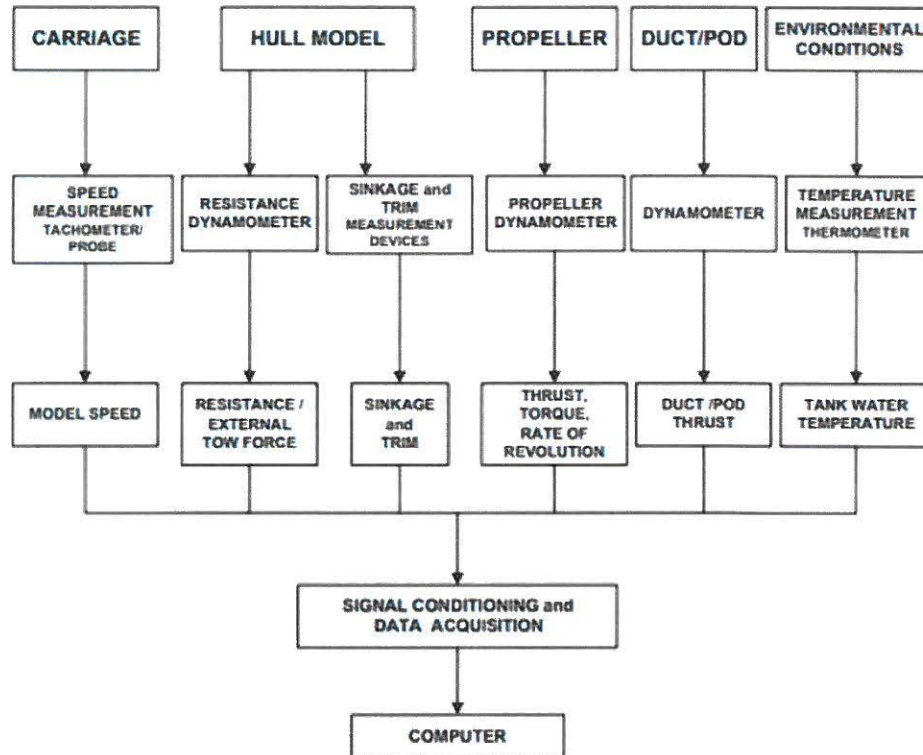


Figure 4-18: Model self-propulsion test setup guidelines from ITTC

In this type of test, the model is connected to a tow carriage through a force sensor, similar to resistance testing. However, rather than the carriage being the sole means of propelling the model, a model propeller is fitted on the ship and instrumented sim-

ilarly to open water propeller testing. The ship is then towed at a variety of different propeller loading factors. This is similar to open water propeller test approach where the propeller rpm is maintained constant and the advance velocity changed to obtain different propeller loading. Prior to conducting the self-propelled testing, the general operating characteristics of the ship propeller must be known. This allows for the load condition of the propeller for each test to be determined. Using the open water propeller test data, this testing can determine if the propeller will operate as expected in the flow stream of the ship to provide the required propulsion.

#### 4.8.2 Modification for Control Authority Testing

When testing the asymmetric propeller, the propulsion was not the primary factor of concern. As such, I had to modify the procedure allow for measurements of the yaw force on the model as it is towed at different speeds. I used the same general procedure as described for self-propulsion tests, but evaluated the yaw moment under different loading condition and up through the maximum expected speed possible for the carriage. The test vehicle was run in two configurations through the same range of speeds. The first utilized only the single bladed propeller to provide control authority. The second configuration used two foils acting as a rudder located forward of the propeller. The two test configurations used are shown in Figure 4-19.

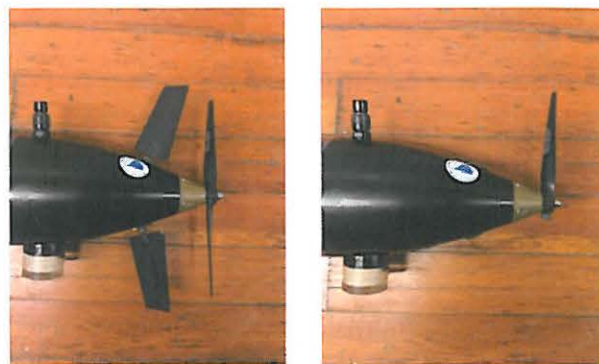


Figure 4-19: Rudder (left) and propeller (right) control systems

In order to measure the yaw forces, the model was attached to a six degree of

freedom force sensor. The sensor was then attached by a strut to the tow carriage. Unlike standard model self-propulsion tests, these trials were being conducting with a full size vehicle which removed the need for scaling. However, due to limitation on the tow carriage, I was only able to tow the UUV at 3.25 knots as compared the full speed it was able to achieve under its own power. While this does not characterize the full operating spectrum of the UUV, it allow me to evaluate the low speed maneuverability which was the operating regime where I expected the transition point to where the rudder becomes more effective than the propeller for steering as seen in Figure 3-5.

For the test setup, I used a piece of T-slotted aluminum to create a mounting bar on the test vehicle. This was attached using stainless steel band clamps which were used to hold the mounting bar was axially aligned with the test vehicle. This was the mounting point for the force sensor used for testing. The test configuration was designed similar to the one used for a low speed maneuverability study. The test configuration used in this experiment is shown in Figure 4-20. In my setup, one of the mounting points was a pin which allowed for free rotation and the other was the force sensor which allowed my to measure the drag and yaw moment.

Similar to the testing described in Reference [3], I measured the yaw force which was developed by the test vehicle in each case. This allowed me to see the control authority for a range of test vehicle speeds and propeller loading conditions. The result would be a graph with empirical results similar to the theoretical values in Figure 3-5.

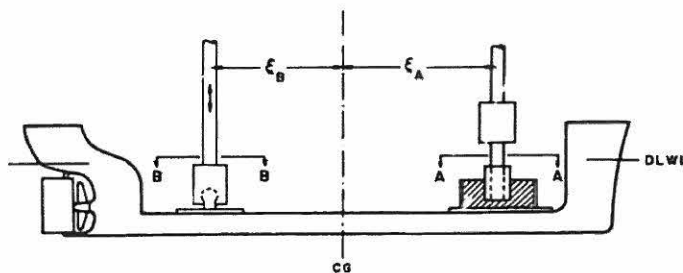


Figure 4-20: Configuration for control authority testing [3]

THIS PAGE INTENTIONALLY LEFT BLANK

# Chapter 5

## Results

### 5.1 Open Water Propeller Test Results

The first phase of the propeller testing was conducted using the aluminum trolling propeller and the propeller boat for the open water performance. During the initial testing for the single blade propeller, the results did not follow the expected trend. As can be seen from the B-series testing results, the point where  $K_t$  crosses the x-axis is function of the pitch of the propeller. The number of blades changes the characteristics of the curve, but the intersection point is driven by geometry. In this round of testing, the x-axis intercept point of the  $K_t$  curve was not consistent between the two propellers. For the pitch of the propeller, the intercept should be close to an advance ratio of 0.6 but was much higher for these trials. When analyzing the first set of results further, I also noticed there was a large variation in the thrust between different runs. Additionally, the torque for single blade variant was higher than that for the two blade variant. These results can be seen in Figure 5-1. This did not make sense since the resistance for the single blade propeller should be less than that for the two blade propeller. Additionally, the amount of scatter in the data made it impossible to calculate a reasonable best fit curve.

After investigating my test setup, I determined that the likely cause of the erratic reading and increased resistance was binding in the propeller shaft due to the imbalance of the propeller. This led to an increase in required torque because of the

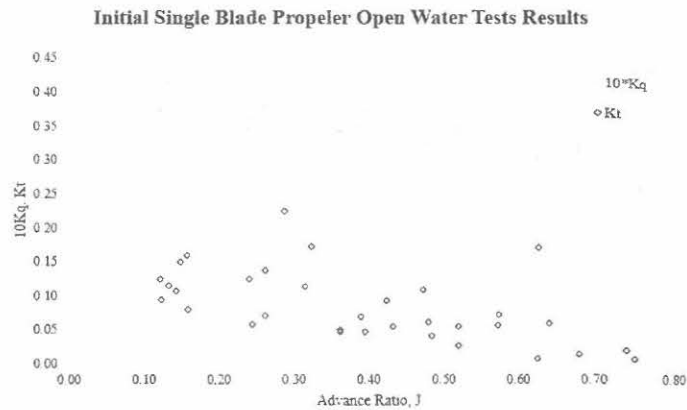


Figure 5-1: Initial test results for single blade propeller

resistance due to binding. Additionally, the thrust is measured based off a deviation from a starting thrust each run. Because of the binding, the decrement during each run was smaller than it should have been resulting in a downward shift of the  $K_t$  curve. The original test vehicle created at WHOI was using an unbalanced propeller without issue, however there were two main factors that exacerbated the imbalance for my testing. The first fact was the material of the propeller. The propeller used by WHOI was plastic where I was using an aluminum propeller, so the magnitude of the eccentric weight was much larger for my test propeller. The second factor was the length of unsupported shaft in each case. The test vehicle propeller was located close to the motor whereas in my test setup I needed adequate separation to ensure smooth inflow for the propeller. This meant that the imbalanced propeller was not supported for approximately 60cm.

The in order to resolve this I had to create a counterweight for the propeller. In order to determine the required weight, I used the blade that was removed to determine the mass and approximate distribution of mass of the blade. Using the known mass and center of mass of the removed propeller blade and the distance to the center of mass for the counterweight, I was able to determine the amount of lead required balance the propeller.

The counterweight was made of lead to reduce the physical size required to obtain

a balanced propeller. I used lead fishing weights to create the counterbalance and cast them onto the hub of the propeller. Once the lead was cast onto the hub of the propeller, it was attached using epoxy as well as two bolts. The lead was then faired in to the hub using epoxy resin to reduce the drag created by the counterweight.

With the reduced vibrations, the results of the open water propeller testing followed the expected performance. The thrust and torque were lower for the single blade propeller as compared to the two bladed propeller. Additionally, the thrust produced went to zero at the same advance ratio for both propellers. The results from both tests are shown in Figure 5-2.

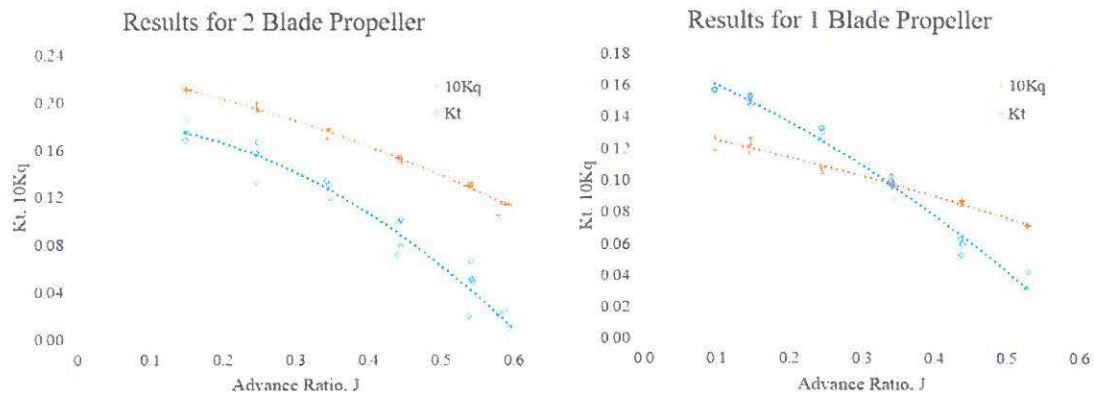


Figure 5-2: Open water test results

The main question was if the torque would reduce faster than the thrust resulting in a higher open water efficiency. The final results in Figure 5-3 show that the torque coefficient was roughly half as much for the single blade propeller as for the two blade propeller for a smaller decrement in thrust resulting in an increased peak efficiency of roughly 13%. All of the parameters are shown in green for the single blade propeller and black for the two blade propeller.

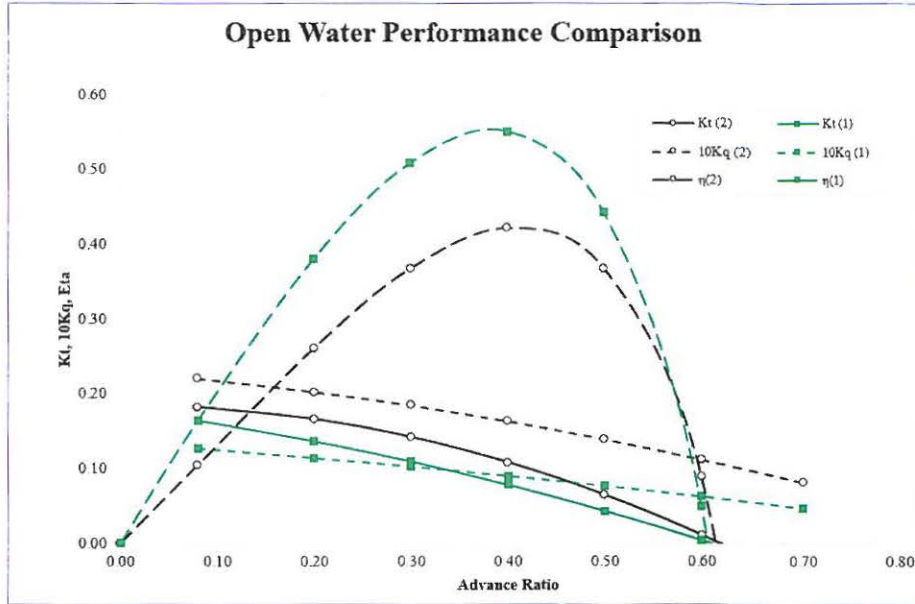


Figure 5-3: Open water performance comparison for one and two blade propellers

## 5.2 Control Authority Results

During the control authority testing I encountered a two issues that precluded collecting definitive data. Initially, the test vehicle was mounted using a single strut similar to submarine resistance testing. This was done to reduce the impact of the flow disturbances from the strut into the propeller and control surfaces. This setup worked for the rudder configuration, however, due to the periodic nature of the steering force for the single blade propeller, it resulted in excessive vibrations of the test vehicle. This was resolved by increasing the rigidity of the structure used to mount the vehicle to the carriage. Once this was resolved, I discovered further issues with the sensor being used to collect data. As with the open water propeller testing, the control authority testing was being conducted with the sensors that were available from previous testing. While the sensor worked when bench tested, once it was connected to the test vehicle in the water, I noticed excessive cross talk between two of the axes. Because the sensor measures force in 3 axes, there is some amount of interference expected between the X and Y axis. However, the amount observed once

the sensor is in the water was beyond the acceptable limit for data collection. As a result it was not possible to obtain reliable data. The sensor was attempted to be repaired but was not returned in time to complete testing. Due to this, I was unable to obtain final results for the control authority portion of testing.

I was able to run the test vehicle in the tank while it was unconstrained to validate the ability to maneuver the test vehicle. Using the MATLAB GUI provided with the test vehicle I was able to successfully steer the test vehicle in both directions.

THIS PAGE INTENTIONALLY LEFT BLANK

# Chapter 6

## Conclusion

### 6.1 Feasibility and Desirability for UUVs

#### 6.1.1 Efficiency

As shown in Chapter 5, the single blade propeller has a higher peak open water efficiency than a similar propeller with two blades. However, to have a comparable comparison the operating point of the propeller needs to be considered. The actual efficiency of the propeller which it is on the UUV will be dependent on the thrust required to obtain a speed. This principle is illustrated in Figure 6-1. In this case it is assumed that the UUV needs a thrust which equates to a  $K_t$  of 0.11 for the two blade propeller, represented by the red line in Figure 6-1. In order to achieve this, the single blade propeller must operate at a different advance ratio which can be calculated by assuming the same advance velocity for both cases and the same thrust.

$$V_{a,1} = V_{a,2} \implies J_{a,1}n_1D_1 = J_{a,2}n_2D_2 \quad (6.1)$$

$$\frac{n_1}{n_2} = \frac{J_{a,2}}{J_{a,1}} \quad (6.2)$$

$$T_1 = T_2 \implies K_{t,1}\rho n_1^2 D^4 = K_{t,2}\rho n_2^2 D^4 \implies K_{t,1}n_1^2 = K_{t,2}n_2^2 \quad (6.3)$$

$$K_{t,2} = K_{t,1} \frac{n_1^2}{n_2^2} = K_{t,1} \frac{J_2^2}{J_1^2} \quad (6.4)$$

$$\text{For this case, } K_{t,1} = 0.11 \quad J_1 = 0.4 \quad (6.5)$$

$$K_{t,2} = -0.2 \cdot J_2^2 - 0.18 \cdot J_2 + 0.18 = J_2^2 \cdot \frac{0.11}{0.4^2} \quad (6.6)$$

$$J_2 = 0.36 \quad (6.7)$$

The resulting operating point for both propellers is shown in Figure 6-1. In this case, the single blade propeller is not operating at its optimal open water efficiency, but is still at a higher efficiency than the similar two blade propeller. The result is that the single blade propeller required a higher rpm by 10% but resulted in approximately 12% higher efficiency. Based on this, a single blade propeller is a valid way to increase the mission capability for a UUV provided that a motor capable of driving it at the required speed is available.

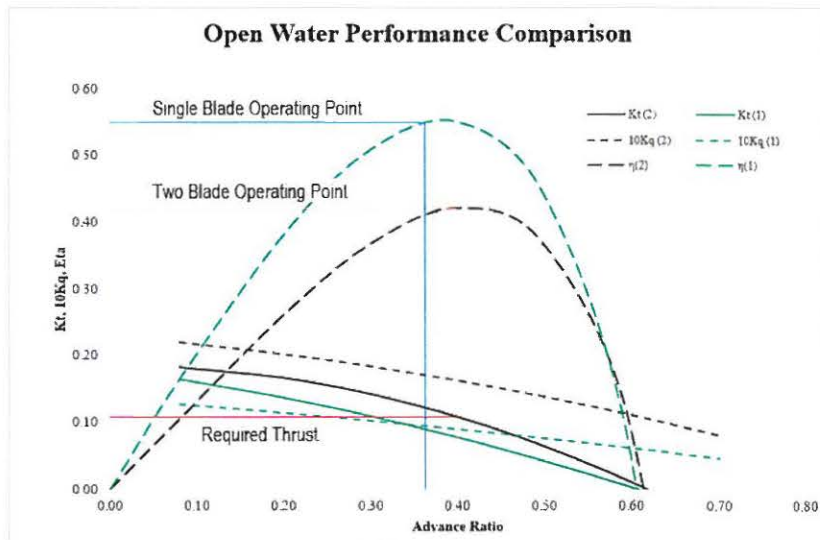


Figure 6-1: Operating point comparison

### **6.1.2 Control Authority**

While I was unable to complete a comparative test between the two methods for control authority, I was able to validate that the single blade propeller was able to steer the UUV through trials in the tow tank. As a result, the technology is feasible to be used for steering a UUV, although the effectiveness compared to a traditional rudder is not yet known.

### **6.1.3 Summary**

Based on the testing that was conducted during this thesis, a single blade propeller is a feasible architecture for future UUVs worth further investigations. In a mission where extended time on station is required, a single blade propeller can provide a means of achieving extra stay time through a higher propulsive efficiency. This could be implemented for UUVs with traditional rudder configurations as well as using the single blade propeller for steering and removing the rudder. While the control authority of the two configurations is not known, in an application where the form factor of the UUV is more important than maneuverability, the single blade propeller is once again a feasible and potentially desirable option. In summary, below are the use cases identified in this thesis for the single blade asymmetric propeller.

1. Must be compatible with existing host vehicle ocean interfaces
2. Needs to be cylindrical in shape with no protrusions
3. Higher efficiency is more important than speed

## **6.2 Future Recommendations**

The single blade propeller showed promise for future UUVs, however, more testing is needed to fully characterize its performance. Three areas for further research into use of asymmetric propellers would include completing control authority testing, use

of multiblade asymmetric propellers, and development of an operational UUV with a single blade propeller.

**Control Authority:** As discussed earlier, a number of use cases for this technology depend on how it compares to a traditional rudder. As such, completing the testing originally intended for this thesis would answer some of the questions of how the two compare. Completing a test program similar to that outlined in Reference [3] would give insight to this aspect of the single blade propeller.

**Multiblade Asymmetric Propellers:** One of the findings was that the single blade propeller generated less thrust than a similar multiblade propeller. However, if the single blade propeller architecture is adopted for superior steering performance instead of just better propulsive efficiency, using multiple blades in an symmetric configuration could yield higher thrust while maintaining the same benefits for maneuverability and form factor.

**Develop Operational UUV:** During my testing I encountered some vibrations of the asymmetric propellers due to force imbalances and the weight imbalance. While the imbalance can be eliminated, the force imbalance will always remain. This could impact the control system of a UUV utilizing an asymmetric propeller as it would have to account for a non uniform force propelling the UUV. This could effect the inertial navigation of the UUV as well as other aspects of its operation such as depth keeping. To date, all of the testing of the single blade UUV has constrained the UUV either to the surface of a test stand which mitigated the effects of this. A future thesis to develop a fully functional, neutrally buoyant UUV could give insight into other potential complications with an asymmetric propeller.

# Appendix A

## Control Authority Estimation

Constants

$\rho$	998 kg/m <sup>3</sup>
span	0.005 m <sup>2</sup>
$C_L$	1
Distance from rudder to center of pressure ( $D_p$ )	0.25 m
Propeller thrust (T)	15.7 N
Propeller radius (r)	0.057 m

Formulas

Lift = $0.5 \cdot \rho \cdot s \cdot C_L$
Turning force (rudder) = Lift * D
Turning force (rudder) = T * r

V	Lift	Turning Force	
		Rudder	Propeller
m/s	N	N-m	N-m
0.00	0.00	0.00	0.90
0.19	0.02	0.01	0.90
0.39	0.10	0.02	0.90
0.58	0.22	0.06	0.90
0.78	0.40	0.10	0.90
0.97	0.62	0.16	0.90
1.17	0.90	0.22	0.90
1.36	1.22	0.31	0.90
1.56	1.60	0.40	0.90
1.75	2.02	0.51	0.90
1.94	2.50	0.62	0.90
2.14	3.02	0.75	0.90
2.33	3.59	0.90	0.90
2.53	4.22	1.05	0.90
2.72	4.89	1.22	0.90
2.92	5.61	1.40	0.90
3.11	6.39	1.60	0.90
3.30	7.21	1.80	0.90
3.50	8.08	2.02	0.90
3.69	9.01	2.25	0.90
4.28	12.08	3.02	0.90
5.83	22.46	5.61	0.90
7.78	39.92	9.98	0.90

## Appendix B

# Propeller Boat Validation Test Results

Va m/s	J -	n rpm	T-Volts V	dT-Volts V	Q-Volts V	dT V	T N	Kt -	Q N-m	Kq -
0.25	0.14	536	-0.040	-0.006	-0.544	-0.7	45.8	0.4	1.45	0.74
0.50	0.28	560	-0.063	0.005	-0.523	0.6	44.5	0.4	1.38	0.64
0.75	0.40	585	-0.243	0.030	-0.499	3.7	41.3	0.3	1.30	0.55
0.75	0.40	583	-0.096	0.023	-0.501	2.9	42.2	0.3	1.30	0.56
1.00	0.51	609	-0.088	0.057	-0.475	7.1	38.0	0.3	1.21	0.48
1.30	0.63	637	-0.068	0.111	-0.439	14.0	31.0	0.2	1.09	0.39
1.60	0.75	657	-0.058	0.133	-0.397	16.8	28.3	0.2	0.94	0.32
0.25	0.14	537	-0.249	-0.038	-0.541	-4.8	49.9	0.5	1.45	0.73
0.50	0.28	555	-0.235	0.031	-0.520	3.9	41.2	0.4	1.37	0.65
0.75	0.40	581	-0.243	0.016	-0.499	2.1	43.0	0.4	1.30	0.56
1.00	0.51	608	-0.209	0.053	-0.473	6.7	38.4	0.3	1.21	0.48
1.30	0.64	632	-0.204	0.084	-0.436	10.5	34.5	0.2	1.08	0.39
1.60	0.76	655	-0.161	0.127	-0.396	16.0	29.1	0.2	0.94	0.32
0.25	0.17	445	-0.185	0.010	-0.412	1.2	32.2	0.4	0.99	0.73
0.50	0.33	467	-0.225	0.029	-0.385	3.6	29.8	0.4	0.90	0.60
0.75	0.47	490	-0.189	0.041	-0.357	5.1	28.3	0.3	0.80	0.49
1.00	0.62	500	-0.151	0.087	-0.325	11.0	22.4	0.2	0.69	0.40
1.30	0.77	521	-0.084	0.143	-0.284	18.1	15.3	0.2	0.55	0.29
1.60	0.92	538	-0.046	0.190	-0.238	23.9	9.5	0.1	0.38	0.19

Va m/s	J -	n rpm	T-Volts V	dT-Volts V	Q-Volts V	dT V	T N	Kt -	Q N-m	Kq -
0.25	0.17	447	-0.206	0.000	-0.406	0.0	33.4	0.5	0.97	0.71
0.50	0.33	470	-0.222	-0.014	-0.384	-1.7	35.1	0.4	0.89	0.59
0.75	0.48	485	-0.219	0.017	-0.354	2.1	31.3	0.4	0.79	0.49
1.00	0.62	503	-0.135	0.064	-0.328	8.1	25.3	0.3	0.70	0.40
1.30	0.77	526	-0.094	0.135	-0.285	17.0	16.4	0.2	0.55	0.29
1.60	0.91	546	-0.081	0.176	-0.238	22.2	11.2	0.1	0.38	0.19
0.25	0.16	486	-0.248	0.020	-0.458	2.5	35.2	0.4	1.15	0.71
0.50	0.31	507	-0.293	0.019	-0.433	2.4	35.4	0.4	1.07	0.61
0.75	0.44	526	-0.297	0.026	-0.405	3.3	34.5	0.3	0.97	0.51
1.00	0.57	544	-0.255	0.081	-0.376	10.3	27.5	0.3	0.87	0.43
1.30	0.72	559	-0.208	0.115	-0.336	14.5	23.3	0.2	0.73	0.34
1.60	0.85	584	-0.141	0.192	-0.291	24.2	13.6	0.1	0.57	0.24
0.25	0.16	490	-0.285	0.028	-0.453	3.5	34.3	0.4	1.14	0.69
0.50	0.31	504	-0.310	0.007	-0.433	0.8	36.9	0.4	1.07	0.61
0.75	0.44	526	-0.310	0.035	-0.411	4.4	33.4	0.3	0.99	0.52
1.00	0.57	547	-0.280	0.085	-0.381	10.7	27.1	0.3	0.88	0.43
1.30	0.71	567	-0.244	0.124	-0.341	15.6	22.2	0.2	0.74	0.34
1.60	0.84	591	-0.170	0.163	-0.292	20.5	17.3	0.1	0.57	0.24

Va m/s	J -	n rpm	T-Volts V	dT-Volts V	Q-Volts V	dT V	T N	Kt -	Q N-m	Kq -
0.25	0.15	520	-0.366	0.018	-0.517	2.2	40.6	0.4	1.36	0.73
0.50	0.28	547	-0.371	-0.011	-0.493	-1.3	44.2	0.4	1.28	0.62
0.75	0.41	563	-0.361	0.038	-0.464	4.8	38.0	0.3	1.17	0.54
1.00	0.53	582	-0.321	0.084	-0.434	10.6	32.3	0.3	1.07	0.46
1.30	0.67	599	-0.264	0.115	-0.396	14.5	28.4	0.2	0.94	0.38
1.60	0.78	635	-0.212	0.179	-0.350	22.6	20.3	0.1	0.78	0.28
0.25	0.15	520	-0.391	0.020	-0.513	2.5	40.4	0.4	1.35	0.73
0.50	0.29	542	-0.401	0.004	-0.491	0.5	42.4	0.4	1.27	0.63
0.75	0.41	565	-0.388	0.043	-0.463	5.4	37.5	0.3	1.17	0.54
1.00	0.53	579	-0.344	0.071	-0.435	9.0	33.9	0.3	1.07	0.47
1.30	0.67	601	-0.313	0.116	-0.393	14.6	28.3	0.2	0.93	0.37
1.60	0.80	622	-0.278	0.161	-0.351	20.3	22.6	0.2	0.78	0.29
0.25	0.14	570	-0.483	0.016	-0.594	2.1	49.0	0.4	1.63	0.73
0.50	0.26	585	-0.508	0.001	-0.573	0.1	51.0	0.4	1.56	0.66
0.75	0.38	613	-0.483	0.028	-0.549	3.5	47.5	0.4	1.47	0.57
1.00	0.49	635	-0.445	0.076	-0.529	9.6	41.5	0.3	1.40	0.51
1.30	0.61	662	-0.426	0.074	-0.494	9.4	41.7	0.3	1.28	0.43
1.60	0.71	697	-0.385	0.150	-0.456	18.9	32.2	0.2	1.15	0.34

Va m/s	J -	n rpm	T-Volts V	dT-Volts V	Q-Volts V	dT V	T N	Kt -	Q N-m	Kq -
0.25	0.14	551	-0.548	-0.031	-0.594	-3.8	54.9	0.5	1.63	0.78
0.25	0.14	563	-0.551	-0.025	-0.580	-3.2	54.3	0.5	1.58	0.73
0.50	0.26	588	-0.531	-0.006	-0.564	-0.8	51.8	0.4	1.52	0.64
0.75	0.38	607	-0.528	0.006	-0.544	0.7	50.3	0.4	1.46	0.58
1.00	0.49	636	-0.487	0.060	-0.525	7.6	43.5	0.3	1.39	0.50
1.30	0.61	659	-0.457	0.053	-0.492	6.6	44.4	0.3	1.27	0.43
1.60	0.72	686	-0.415	0.139	-0.452	17.6	33.5	0.2	1.13	0.35
1.60	1.01	483	-0.217	0.170	-0.188	21.5	5.8	0.1	0.21	0.13
1.60	1.01	492	-0.235	0.161	-0.186	20.2	7.0	0.1	0.20	0.12

THIS PAGE INTENTIONALLY LEFT BLANK

## Appendix C

### Single Blade Propeller Test Results

Two Blade Propeller Results

Va m/s	J -	n rpm	T Volts	dT Volts	Q Volts	Thrust N	Kt -	Torque N-m	10Kq -
1.3	0.634	734	-0.191	0.211	0.161	-2.2	-0.02	0.20	0.10
1.3	0.636	732	-0.193	0.220	0.162	-3.3	-0.03	0.20	0.10
1.3	0.632	736	-0.171	0.170	0.164	3.0	0.02	0.21	0.11
1.2	0.583	736	-0.203	0.193	0.169	-0.1	0.00	0.23	0.12
1.2	0.588	731	-0.206	0.170	0.168	2.8	0.02	0.23	0.11
1.2	0.592	725	-0.190	0.184	0.166	1.1	0.01	0.22	0.11
1.2	0.579	741	-0.179	0.172	0.164	2.7	0.02	0.21	0.11
0.3	0.150	718	-0.291	0.027	0.211	21.0	0.19	0.40	0.21
0.3	0.148	726	-0.294	0.038	0.213	19.5	0.17	0.41	0.21
0.3	0.149	722	-0.318	0.035	0.212	20.0	0.18	0.40	0.21
0.7	0.342	733	-0.271	0.068	0.195	15.7	0.13	0.33	0.17
0.7	0.346	723	-0.262	0.084	0.196	13.7	0.12	0.34	0.18
0.7	0.347	723	-0.259	0.075	0.196	14.9	0.13	0.34	0.18
0.9	0.444	725	-0.222	0.120	0.183	9.1	0.08	0.29	0.15
0.9	0.445	725	-0.244	0.101	0.186	11.7	0.10	0.30	0.16
0.9	0.441	730	-0.247	0.101	0.187	11.6	0.10	0.30	0.15
0.9	0.441	731	-0.219	0.126	0.186	8.4	0.07	0.30	0.15
1.1	0.539	731	-0.182	0.174	0.175	2.4	0.02	0.25	0.13
1.1	0.542	726	-0.177	0.146	0.176	5.9	0.05	0.26	0.13
1.1	0.540	728	-0.175	0.132	0.175	7.7	0.07	0.25	0.13
1.1	0.544	724	-0.174	0.149	0.174	5.6	0.05	0.25	0.13
0.5	0.248	722	-0.295	0.042	0.204	19.0	0.17	0.37	0.19
0.5	0.246	726	-0.305	0.049	0.206	18.1	0.16	0.38	0.20
0.5	0.246	729	-0.300	0.070	0.208	15.5	0.13	0.39	0.20
1.3	0.639	728	-0.193	0.219	0.160	-3.2	-0.03	0.19	0.10

One Blade Propeller Results

Va m/s	J -	n rpm	T Volts	dT Volts	Q Volts	Thrust N	Kt -	Torque N-m	10*Kq -
0.2	0.097	734	-0.357	0.014	0.165	18.5	0.16	0.23	0.12
0.2	0.097	736	-0.381	0.014	0.170	18.6	0.16	0.25	0.13
0.5	0.244	732	-0.353	0.038	0.160	15.6	0.13	0.21	0.11
0.5	0.241	687	-0.277	0.050	0.159	14.1	0.14	0.21	0.12
0.5	0.243	731	-0.289	0.030	0.160	16.6	0.14	0.21	0.11
1.1	0.527	737	-0.192	0.119	0.143	5.3	0.04	0.15	0.07
1.1	0.528	737	-0.209	0.114	0.141	6.1	0.05	0.14	0.07
0.9	0.436	739	-0.248	0.102	0.149	7.5	0.06	0.17	0.08
0.9	0.438	735	-0.296	0.106	0.149	7.0	0.06	0.17	0.09
0.7	0.342	733	-0.326	0.072	0.154	11.3	0.10	0.19	0.10
0.7	0.344	729	-0.306	0.081	0.154	10.2	0.09	0.19	0.10
0.5	0.243	736	-0.356	0.045	0.159	14.7	0.12	0.21	0.11
1.1	0.147	731	-0.143	0.020	0.168	17.9	0.15	0.25	0.13
0.9	0.146	736	-0.133	0.021	0.165	17.7	0.15	0.23	0.12
0.9	0.146	734	-0.130	0.024	0.167	17.3	0.15	0.24	0.12
1.3	0.147	731	-0.125	0.019	0.169	17.9	0.15	0.25	0.13
0.3	0.340	737	-0.091	0.065	0.158	12.2	0.10	0.21	0.10
0.3	0.340	737	-0.091	0.068	0.155	11.8	0.10	0.19	0.10
0.3	0.342	733	-0.007	0.071	0.154	11.5	0.10	0.19	0.10
0.9	0.246	727	-0.009	0.042	0.157	15.1	0.13	0.20	0.10
1.1	0.527	747	0.036	0.131	0.143	3.9	0.03	0.15	0.07
1.1	0.529	744	0.026	0.121	0.143	5.2	0.04	0.14	0.07

THIS PAGE INTENTIONALLY LEFT BLANK

# Bibliography

- [1] ITTC. ITTC - Recommended Procedures and Guidelines: Testing and Extrapolation Methods, Propulsor Open Water Test. Technical report, International Towing Tank Conference, 2002.
- [2] Katie Jacobson. Transforming 'Distributed Lethality' Strategy into Action. <https://www.rand.org/blog/2016/02/transforming-distributed-lethality-strategy-into-action.html>, February 2016.
- [3] C. Lincoln Crane Jr. Response of Slowly Moving Ship to Propeller and Rudder Actions. Technical Report 1169, Davidson Library, David Taylor Model Basin, October 1966.
- [4] OPNAV N97. The Navy Unmanned Undersea Vehicle Master Plan, November 2004.
- [5] Eric Rebentisch. MIT Course EM.411 Requirements Analysis and Definition, 2017.
- [6] Thomas Rowden, Peter Gumataotao, and Peter Fanta. 'Distributed Lethality'. <https://www.usni.org/magazines/proceedings/2015/january/distributed-lethality>, January 2015.
- [7] Goldman Sachs. Drones: Reporting for Work. <http://www.goldmansachs.com/insights/technology-driving-innovation/drones/>, 2019.
- [8] John Schuster. Robotics in Undersea Warfare, May 2009.

